NASA/TM–20230011547

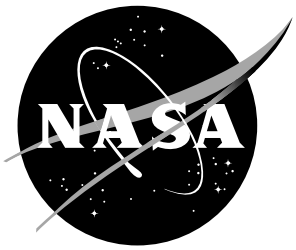

Elastic Modulus Testing for TriTruss Struts

Lauren Simmons
Structural Mechanics and Concepts Branch
Langley Research Center, Hampton, Virginia

October 2023

NASA STI Program Report Series

Since its founding, NASA has been dedicated to the advancement of aeronautics and space science. The NASA scientific and technical information (STI) program plays a key part in helping NASA maintain this important role.

The NASA STI program operates under the auspices of the Agency Chief Information Officer. It collects, organizes, provides for archiving, and disseminates NASA's STI. The NASA STI program provides access to the NTRS Registered and its public interface, the NASA Technical Reports Server, thus providing one of the largest collections of aeronautical and space science STI in the world. Results are published in both non-NASA channels and by NASA in the NASA STI Report Series, which includes the following report types:

- TECHNICAL PUBLICATION. Reports of completed research or a major significant phase of research that present the results of NASA Programs and include extensive data or theoretical analysis. Includes compilations of significant scientific and technical data and information deemed to be of continuing reference value. NASA counterpart of peer-reviewed formal professional papers but has less stringent limitations on manuscript length and extent of graphic presentations.
- TECHNICAL MEMORANDUM. Scientific and technical findings that are preliminary or of specialized interest, e.g., quick release reports, working papers, and bibliographies that contain minimal annotation. Does not contain extensive analysis.
- CONTRACTOR REPORT. Scientific and technical findings by NASA-sponsored contractors and grantees.
- CONFERENCE PUBLICATION. Collected papers from scientific and technical conferences, symposia, seminars, or other meetings sponsored or co-sponsored by NASA.
- SPECIAL PUBLICATION. Scientific, technical, or historical information from NASA programs, projects, and missions, often concerned with subjects having substantial public interest.
- TECHNICAL TRANSLATION. English-language translations of foreign scientific and technical material pertinent to NASA's mission.

Specialized services also include organizing and publishing research results, distributing specialized research announcements and feeds, providing information desk and personal search support, and enabling data exchange services.

For more information about the NASA STI program, see the following:

- Access the NASA STI program home page at http://www.sti.nasa.gov
- Help desk contact information:

https://www.sti.nasa.gov/sti-contact-form/ and select the "General" help request type.

NASA/TM–20230011547

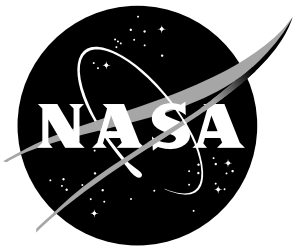

Elastic Modulus Testing for TriTruss Struts

Lauren Simmons
Structural Mechanics and Concepts Branch
Langley Research Center, Hampton, Virginia

National Aeronautics and
Space Administration

Langley Research Center
Hampton, Virginia 23681-2199

October 2023

Available from:

NASA STI Program / Mail Stop 148
NASA Langley Research Center
Hampton, VA 23681-2199
Fax: 757-864-6500

Abstract

The TriTruss is a novel structural module developed by researchers at NASA Langley Research Center (LaRC) that can be used in space to assemble large backing structures for a variety of applications. One such application is the metering truss and primary mirror backbone support structure of an in-space assembled telescope (iSAT). For the iSAT application, the TriTruss will be supporting mirror segments, payloads, and instruments, all of which require the TriTruss to have robust structural integrity. An accurate elastic modulus value is crucial to the finite element analysis (FEA) of the structure. Initial testing indicated that the equivalent elastic modulus provided by the manufacturer and used in the analyses did not accurately predict the behavior of the structure. In this paper, the in-house testing method developed at LaRC to accurately measure the equivalent elastic modulus of the composite struts for use in the analyses is described. A tensile and compressive equivalent elastic modulus was computed from the data obtained in this test. The testing resulted in a tensile equivalent elastic modulus of 24.6 Msi (standard deviation of 0.888 Msi) or 169 GPa (standard deviation of 6.20 GPa) and a compressive equivalent elastic modulus of 22.8 Msi (standard deviation of 0.780 Msi) or 157 GPa (standard deviation of 5.38 GPa) for the single wall thickness struts. For double wall thickness struts, the testing resulted in a tensile equivalent elastic modulus of 32.1 Msi (standard deviation of 1.003 Msi) or 221 GPa (standard deviation of 6.91 GPa) and a compressive equivalent elastic modulus of 31.9 Msi (standard deviation of 1.123) or 220 GPa (standard deviation of 7.74 GPa).

Contents

List of Figures

List of Tables

Nomenclature

a	Length of face triangle strut, m
H	TriTruss module depth, m
L_b	Length of batten member, m
L_c	Length of central triangle strut, m
d_s	Diameter of strut, m

1 Introduction

Space operations are beginning to leverage modular systems and repeated robotic visits to "Persistent Assets", enabling asset maintenance, repair, and enhancement. A "Persistent Asset" (PA) is defined as any near zero-gravity (zero-g) or planetary surface system that benefits from multiple visits [1]. These visits can be used for assembly, servicing, repairs, reconfiguration, and upgrades [2–6]. A key attribute to include when developing such systems is to design them to be modular. The efficiency and robustness of on-orbit assembly operations can be maximized by co-designing modular structures, such as the TriTruss [7], and their associated connectors for robotic handling and joining. One example of a PA that is currently being considered is the In-Space Assembled Telescope (iSAT) shown in Fig. 1.

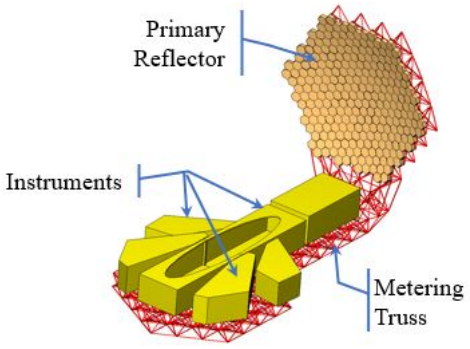

Figure 1: Large in-space assembled telescope [7].

A study was conducted in 2019 [8, 9] that determined the feasibility of designing a large space telescope, the iSAT, and concluded that in order to achieve large apertures (>15-meter diameter primary aperture), robotic in-space assembly of modular components was necessary. The study also concluded that the foundational structure for the telescope, consisting of the metering truss and the primary mirror support truss, should be assembled from modular truss elements that could be packaged prior to launch, deployed on-orbit, and robotically assembled into the final configuration. The truss structure is illustrated in Fig. 2a. Although a specific truss design was not selected during the study, the iSAT structures team baselined the modular TriTruss system for the telescope foundational structure [10].

The TriTruss [7] was developed by researchers at NASA Langley Research Center (LaRC) for systems with triangular or hexagonal topologies, that are flat or curved, such as telescopes and other platforms (see Fig. 2b). The TriTruss has equilateral triangular faces at the top, bottom, and middle. The top triangular face is smaller than the bottom face of the truss when used to support curved surfaces such as telescope primary mirror support structures. The TriTruss has many innovative attributes including design versatility, compact packaging abilities, robotically actuated deployment, and multiple locations for payload attachment. The TriTruss concept was first introduced in Ref. [7] where the details of its design parameters and structural configuration were described.

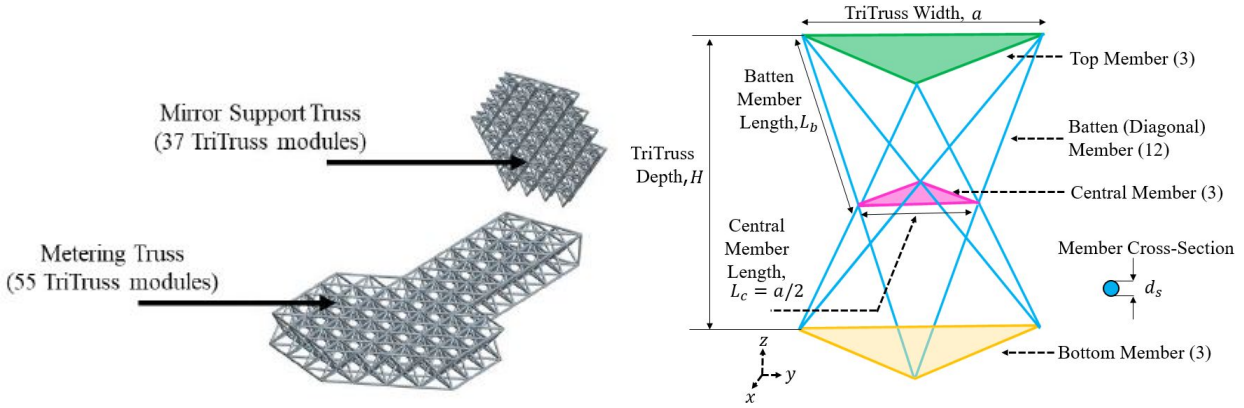

(a) Foundational support structure of an iSAT (b) Geometry and parameters of a TriTruss module

Figure 2: The foundational truss structure of an iSAT assembled from individual TriTruss modules.

In Ref. [7], many different mission applications for the TriTruss are discussed, including a 20-meter diameter space telescope and a beam-type platform that can be used to host payloads and instruments. The geometry and various design variables for the TriTruss are also described. The TriTruss module geometry consists of top- and bottom-face equilateral triangles (strut length, a) with an equilateral central triangle (strut length, $a/2$) located halfway between the two faces. Core struts with length, L_b, (that depend on truss depth, H) connect the central triangle with the face triangles [10]. Bonded joints will be used to connect struts to corner fittings to form the TriTruss. The TriTruss struts are commercial-off-the-shelf (COTS) struts that researchers at LaRC are using in finite element modeling to predict the structural performance. Since only an approximate elastic modulus was provided for the TriTruss composite struts, testing was performed to obtain the tensile and compressive equivalent elastic modulus to provide more accurate data for conducting analysis. Test results are documented and described in this paper for a single wall thickness strut and a double wall thickness strut. The struts are manufactured in a roll-wrapped carbon/epoxy and the single wall material layup is [0/90/90/0] and the double wall material layup is [0/90/90/0/0/90/90/0]. The double wall thickness strut accounts for TriTrusses that are made to be placed in a metering truss or mirror support truss where stiffer structure is required.

2 Test Set Up and Results

The purpose of this test was to estimate the equivalent elastic modulus for composite struts used in a TriTruss. The equivalent elastic modulus was originally provided by the manufacturer, but disagreement between FEA results using the manufacturer-determined elastic modulus and experimental measurements in a TriTruss bond test [11] suggested that the provided elastic modulus may have been inaccurate. After further investigation, it was determined that the elastic modulus test performed by a subcontractor of the manufacturer was unsatisfactory because only one strain gage was applied to each test specimen, the test specimen appeared to be too short, and too few repeat trials were performed. The results documented in this paper were obtained by applying improved elastic modulus determination best practices by conducting more test trials of longer specimens with more strain gages. A tensile and compressive equivalent elastic modulus was computed from the data obtained in this test. One single wall thickness strut and one double wall thickness strut was cut into five specimens, each one at 12 inches in length, for the test. They were each loaded up to 1500 lbs in tension and 1500 lbs in compression at a rate of 4 lbs/sec for the

single wall thickness struts and a rate of 10 lbs/sec for the double wall thickness struts. The struts were loaded and unloaded through this range three times. An aluminum end fitting was bonded to the inside of the strut on both ends using an adhesive and mounted in the test stand. The specimen was pinned using a clevis on both ends. Three strain gages were placed at the center of each strut, equally spaced around the circumference. This test set up is shown in Fig. 3. Testing was conducted in a 50-kip MTS load frame with an inline 5-kip load cell. The inline load cell was calibrated through the MTS FlexTest 40 control system and was set up as a load-control channel. A Micro-Measurements System 7000 data acquisition system was used for collecting load and strain gage data. The data acquisition system was configured with a minimum of eight high level channels for the load and stroke and eight strain gage channels.

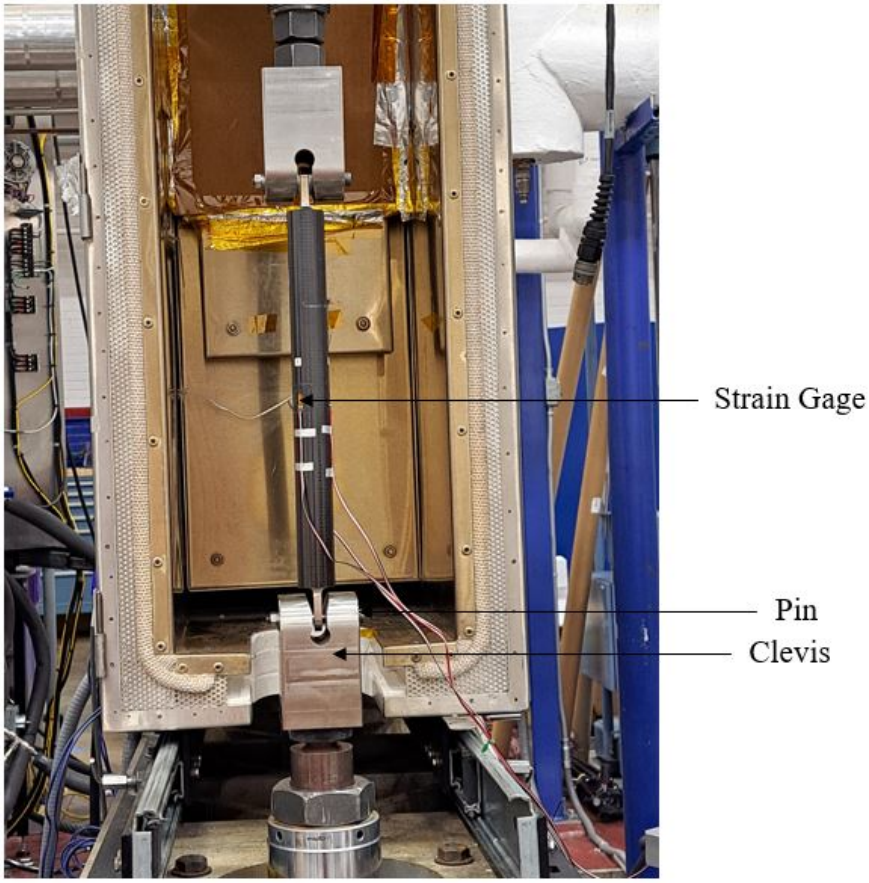

Figure 3: Modulus test set up.

2.1 Single Wall Thickness Struts

The data summarizing the tension modulus data for the single wall thickness strut is shown in Table 1. The five specimens were labeled A, B, C, D, E and have data collected for three trials. Each trial recorded in the table was the average of the three strain gages in that trial. Each of these trials were averaged per specimen and then an overall average value was computed from each of the average specimen values. The stress versus microstrain plot of this is shown in Fig. 4 for all five samples. This results in a tensile equivalent elastic modulus of 24.6 Msi or 169 GPa. The manufacturer of the struts provided a tensile equivalent elastic modulus of 202 GPa. The same procedure was done to compute the compressive equivalent elastic modulus which resulted

in 22.8 Msi or 157 GPa. The manufacturer of the struts provided a compressive equivalent elastic modulus of 142 GPa. The stress versus microstrain plot of this is shown in Fig. 5 for all five samples. These results are summarized in Table 2. Detailed plots showing each individual trial for all five specimens are shown in Appendix A. All trials gave linear data with an excellent line of fit and high R^2 values and the slope of that line was recorded as the modulus for that given trial. The results from all three trials for each specimen were consistent, indicating that the first trial didn't influence the properties determined from the second and third trials.

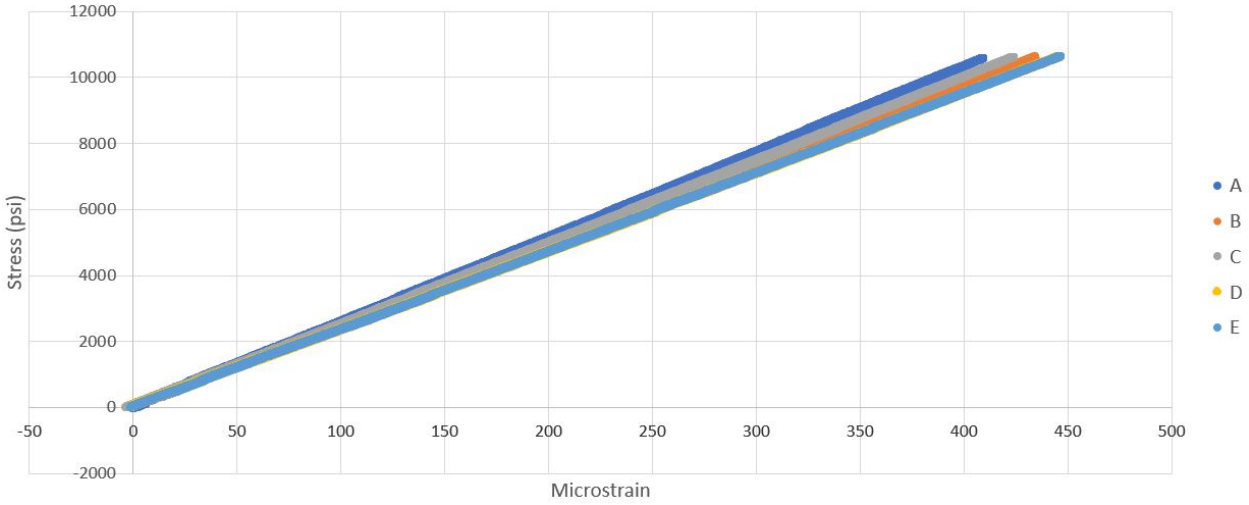

Figure 4: Average equivalent tension elastic modulus for single wall thickness strut.

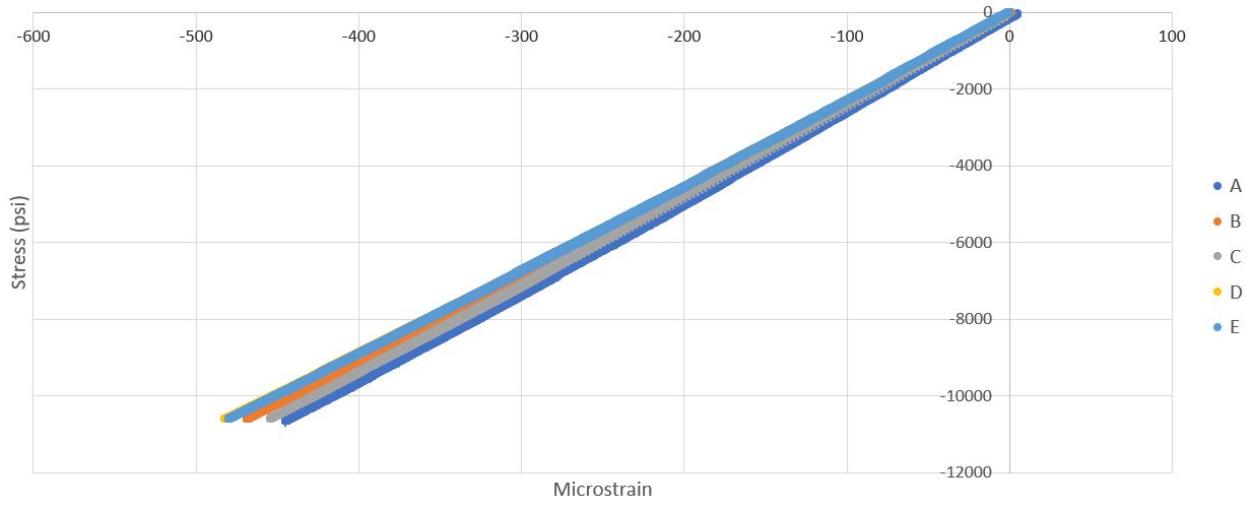

Figure 5: Average equivalent compression elastic modulus for single wall thickness strut.

Table 1: Tension equivalent elastic modulus data for single wall thickness strut.

Specimen	Trial 1 (Msi)	Trial 2 (Msi)	Trial 3 (Msi)	Average (Msi)
A	25.776	25.906	25.903	25.862
B	24.460	24.415	24.439	24.438
C	24.941	24.971	24.977	24.963
D	23.702	23.789	23.746	23.746
E	23.806	23.805	23.715	23.775
Avg	-	-	-	24.557

Table 2: Compression equivalent elastic modulus data for single wall thickness strut.

Specimen	Trial 1 (Msi)	Trial 2 (Msi)	Trial 3 (Msi)	Average (Msi)
A	23.876	23.751	23.820	23.816
B	22.702	22.643	22.643	22.663
C	23.317	23.357	23.320	23.331
D	22.012	21.979	22.056	22.016
E	22.138	22.030	22.139	22.102
Avg	-	-	-	22.786

2.2 Double Wall Thickness Struts

The data summarizing the tension modulus data for the double wall thickness strut is shown in Table 3. The five specimens were labeled A_{dw}, B_{dw}, C_{dw}, D_{dw}, E_{dw} and have data collected for three trials. Each trial recorded in the table was the average of the three strain gages in that trial. Each of these trials were averaged per specimen and then an overall average value was computed from each of the average specimen values. The stress versus microstrain plot of this is shown in Fig. 6 for all five samples. This plot results in a tensile equivalent elastic modulus of 32.1 Msi or 221 GPa. The manufacturer of the struts provided a tensile equivalent elastic modulus of 245 GPa. The same procedure was done to compute the compressive equivalent elastic modulus which resulted in 31.9 Msi or 220 GPa. The manufacturer of the struts provided a compressive equivalent elastic modulus of 159 GPa. The stress versus microstrain plot of this is shown in Fig. 7 for all five samples. These results are summarized in Table 4. Detailed plots showing each individual trial for all five specimens are shown in Appendix B. All trials gave linear data with an excellent line of fit and high R^2 values and the slope of that line was recorded as the modulus for that given trial. The results from all three trials for each specimen were consistent, indicating that the first trial didn't influence the properties determined from the second and third trials.

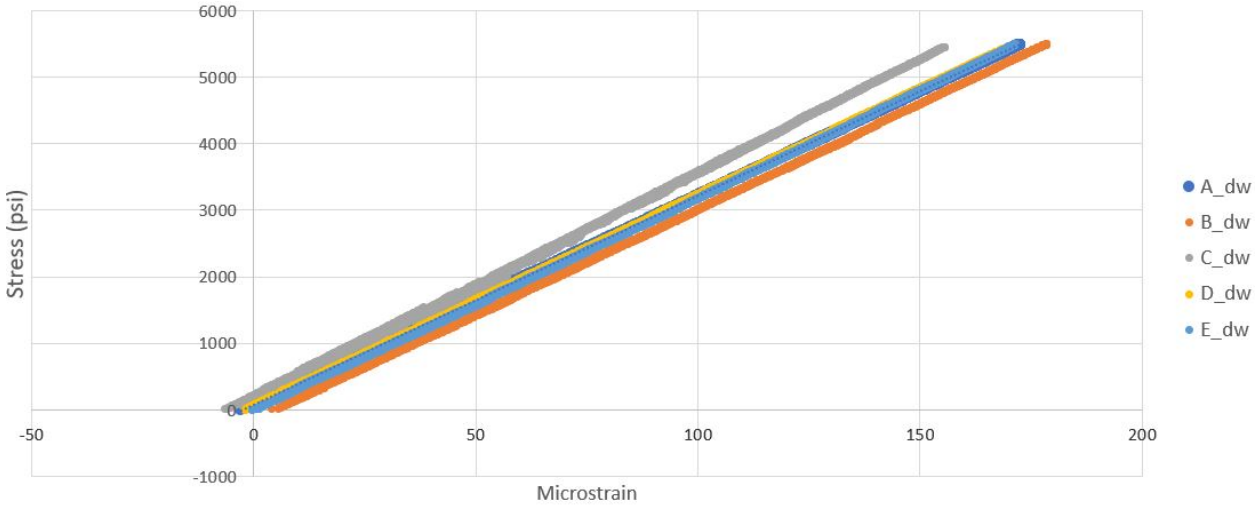

Figure 6: Average equivalent tension elastic modulus for double wall thickness strut.

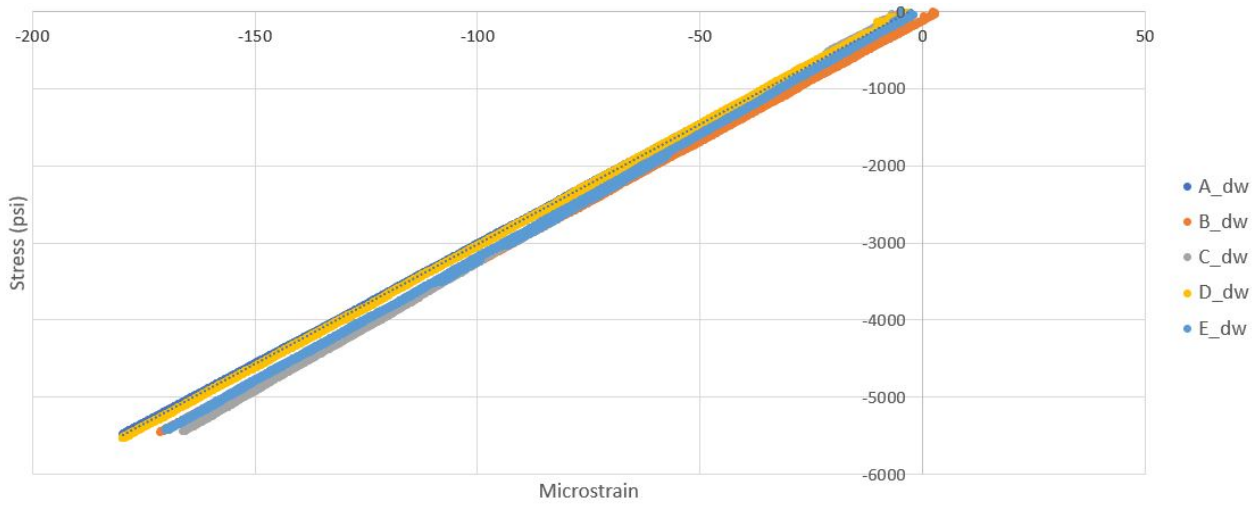

Figure 7: Average equivalent compression elastic modulus for double wall thickness strut.

Table 3: Tension equivalent elastic modulus data for double wall thickness strut.

Specimen	Trial 1 (Msi)	Trial 2 (Msi)	Trial 3 (Msi)	Average (Msi)
A_{dw}	31.250	31.375	31.255	31.293
B_{dw}	31.602	31.537	31.689	31.609
C_{dw}	34.017	33.652	33.856	33.842
D_{dw}	31.807	31.779	31.827	31.804
E_{dw}	32.097	32.009	31.908	32.005
Avg	-	-	-	32.111

Table 4: Compression equivalent elastic modulus data for double wall thickness strut.

Specimen	Trial 1 (Msi)	Trial 2 (Msi)	Trial 3 (Msi)	Average (Msi)
A_{dw}	31.030	30.975	31.050	31.018
B_{dw}	31.326	31.311	31.283	31.307
C_{dw}	33.676	33.794	33.847	33.772
D_{dw}	31.307	31.241	31.307	31.285
E_{dw}	31.924	32.284	32.022	32.077
Avg	-	-	-	31.892

3 Conclusions

Testing was performed to determine the equivalent tensilve and compressive elastic modulus for TriTruss struts to provide more accurate data for conducting various analyses involving the struts. Single wall thickness and double wall thickness struts were tested and analyzed in a similar manner, and an equivalent modulus for tension and compression was computed for both types of struts from the data documented in this paper. All trials gave linear data with an excellent line of fit and the slope of that line was recorded as the modulus for that given trial. The recorded moduli were averaged among all trials and specimens to give an overall equivalent elastic modulus. The testing resulted in a tensile equivalent elastic modulus of 24.6 Msi (standard deviation of 0.888 Msi) or 169 GPa (standard deviation of 6.20 GPa) and a compressive equivalent elastic modulus of 22.8 Msi (standard deviation of 0.780 Msi) or 157 GPa (standard deviation of 5.38 GPa) for the single wall thickness struts. For double wall thickness struts, the testing resulted in a tensile equivalent elastic modulus of 32.1 Msi (standard deviation of 1.003 Msi) or 221 GPa (standard deviation of 6.91 GPa) and a compressive equivalent elastic modulus of 31.9 Msi (standard deviation of 1.123) or 220 GPa (standard deviation of 7.74 GPa). These values can be used in all analyses involving these struts.

Acknowledgments

This research was funded by the Precision Assembled Space Structures (PASS) project. The author would like to acknowledge Ms. Judith Watson (NASA LaRC) for discussions regarding the test set up and execution. The author would also like to acknowledge Mr. Clarence Stanfield (NASA LaRC) for providing test support.

References

1. Doggett, W. R., Dorsey, J., Teter, J., Paddock, D., Jones, T., Komendera, E. E., Bowman, L., Taylor, C., and Mikulas, M., "Persistent Assets in Zero-G and on Planetary Surfaces: Enabled by Modular Technology and Robotic Operations," *2018 AIAA SPACE and Astronautics Forum and Exposition*, American Institute of Aeronautics and Astronautics, Orlando, FL, 2018. https://doi.org/10.2514/6.2018-5305, URL https://arc.aiaa.org/doi/10.2514/6.2018-5305.

2. Dorsey, J. T., "Framework for Defining and Assessing Benefits of a Modular Assembly Design Approach for Exploration Systems," *AIP Conference Proceedings*, Vol. 813, AIP, Albuquerque, New Mexico (USA), 2006, pp. 969–981. https://doi.org/10.1063/1.2169278, URL http://aip.scitation.org/doi/abs/10.1063/1.2169278, iSSN: 0094243X.

3. Belvin, W. K., Dorsey, J. T., and Watson, J. J., "Technology Challenges and Opportunities for Very Large In-Space Structural Systems," 2009, p. 27.

4. Dorsey, J., Doggett, W., Hafley, R., Komendera, E., Correll, N., and King, B., "An Efficient and Versatile Means for Assembling and Manufacturing Systems in Space," *AIAA SPACE 2012 Conference & Exposition*, American Institute of Aeronautics and Astronautics, Pasadena, California, 2012. https://doi.org/10.2514/6.2012-5115, URL http://arc.aiaa.org/doi/10.2514/6.2012-5115.

5. Dorsey, J., and Watson, J., "Space Assembly of Large Structural System Architectures (SALSSA)," *AIAA SPACE 2016*, American Institute of Aeronautics and Astronautics, Long Beach, California, 2016. https://doi.org/10.2514/6.2016-5481, URL http://arc.aiaa.org/doi/10.2514/6.2016-5481.

6. Belvin, W. K., Doggett, W. R., Watson, J. J., Dorsey, J. T., Warren, J. E., Jones, T. C., Komendera, E. E., Mann, T., and Bowman, L. M., "In-Space Structural Assembly: Applications and Technology," *3rd AIAA Spacecraft Structures Conference*, American Institute of Aeronautics and Astronautics, San Diego, California, USA, 2016. https://doi.org/10.2514/6.2016-2163, URL http://arc.aiaa.org/doi/10.2514/6.2016-2163.

7. Doggett, W. R., "TriTruss: A New and Novel Structural Concept Enabling Modular Space Telescopes and Space Platforms," Washington, D.C., 2019.

8. Mukherjee, R., Siegler, N., and Thronson, H., "The Future of Space Astronomy will be Built: Results from the In-Space Astronomical Telecope (iSAT) Assembly Design Study," Washington, D.C., 2019.

9. Siegler, N., Mukherjee, R., and Thronson, H., "NASA-Chartered In-Space Assembled Telescope Study: Final Report," July 2019, https://exoplanets.nasa.gov/internal_resources/1262/, Accessed 4 November 2019.

10. Cline, J., Raffanello, L. M., Song, K., White, B., McGlothin, G. S., Dorsey, J., Doggett, W. R., Mukhopadhyay, R., and Wong, I., "TriTruss Packaging and Deployment Trade Study," *ASCEND 2020*, American Institute of Aeronautics and Astronautics, Virtual Event, 2020. https://doi.org/10.2514/6.2020-4128, URL https://arc.aiaa.org/doi/10.2514/6.2020-4128.

11. Simmons, L., and Song, K., "Testing of Bonds in a TriTruss Module," *AIAA SCITECH 2023 Forum*, 2023, p. 1700.

Appendix A

Single Wall Thickness Strut Stress vs. Strain Plots

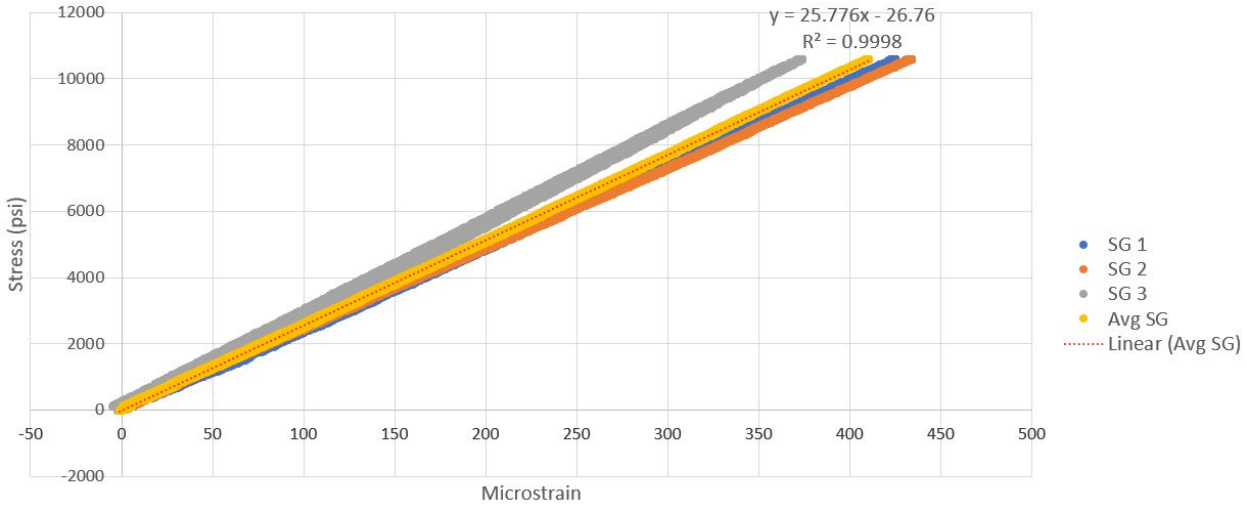

Figure A1: Specimen A, tension trial 1.

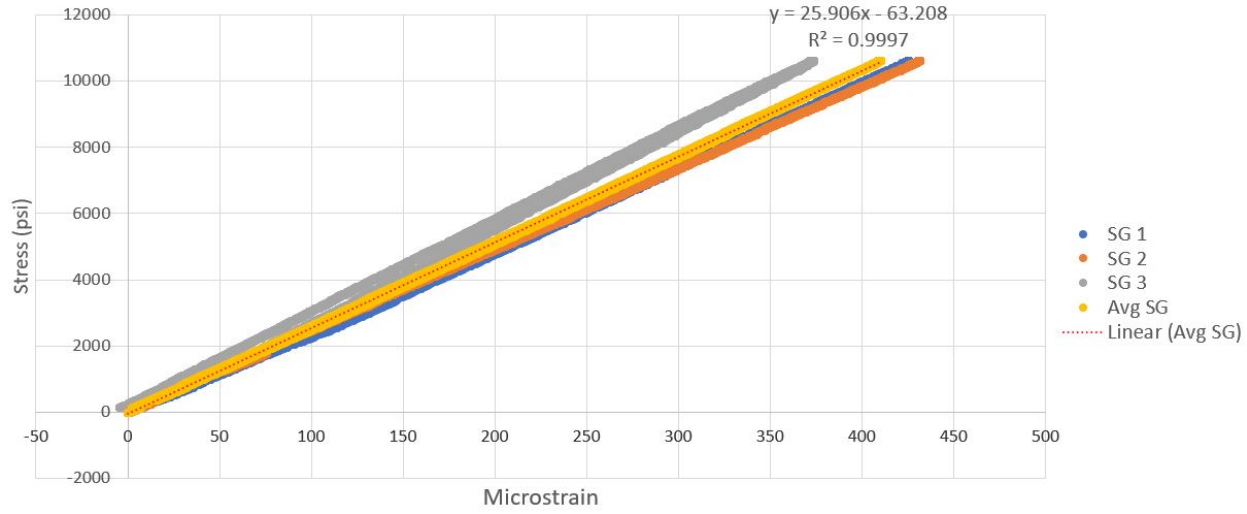

Figure A2: Specimen A, tension trial 2.

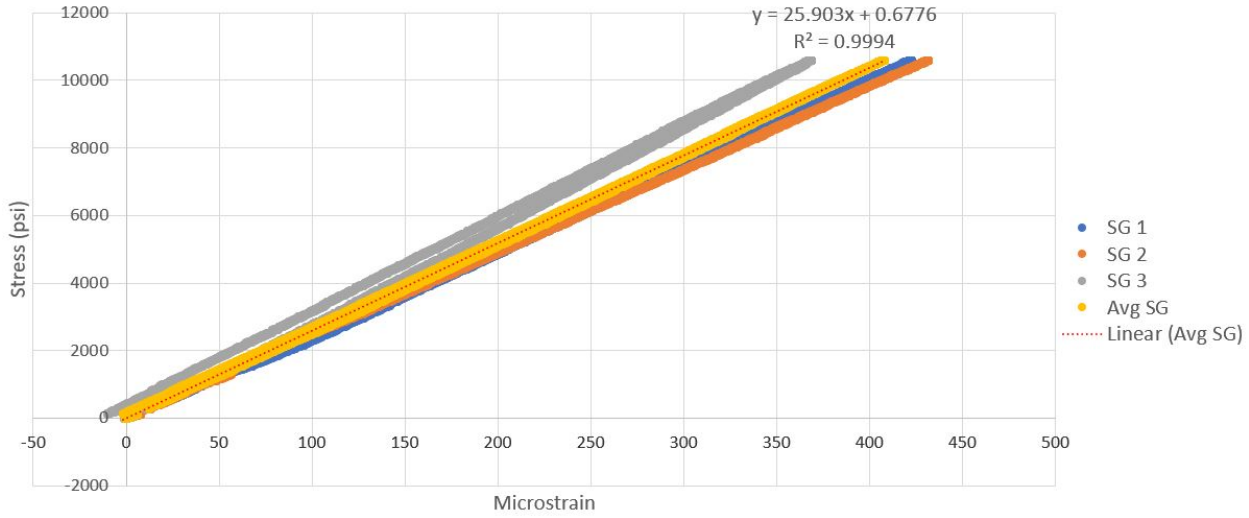

Figure A3: Specimen A, tension trial 3.

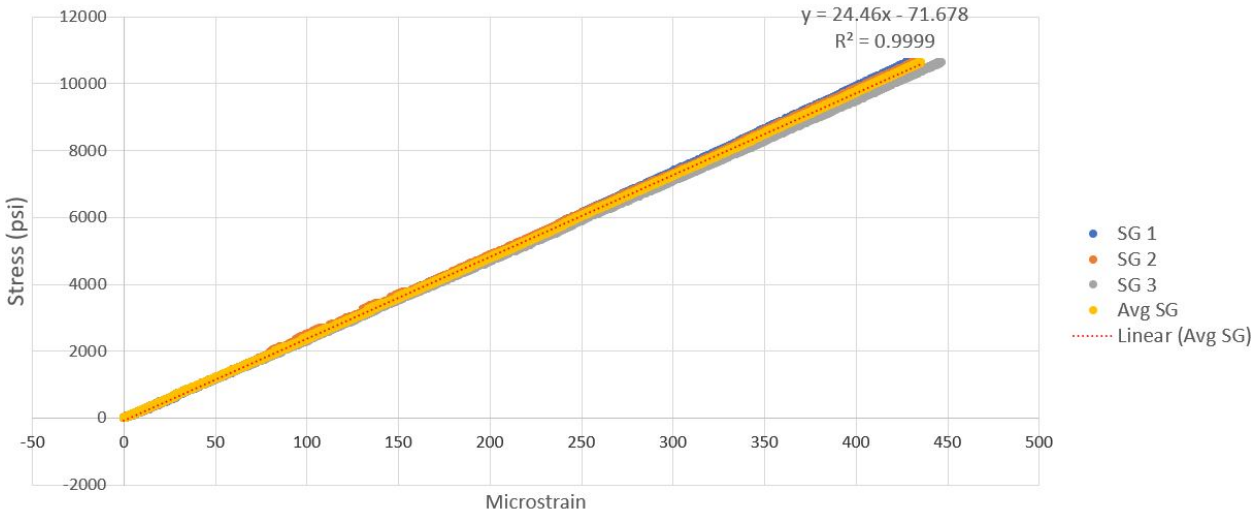

Figure A4: Specimen B, tension trial 1.

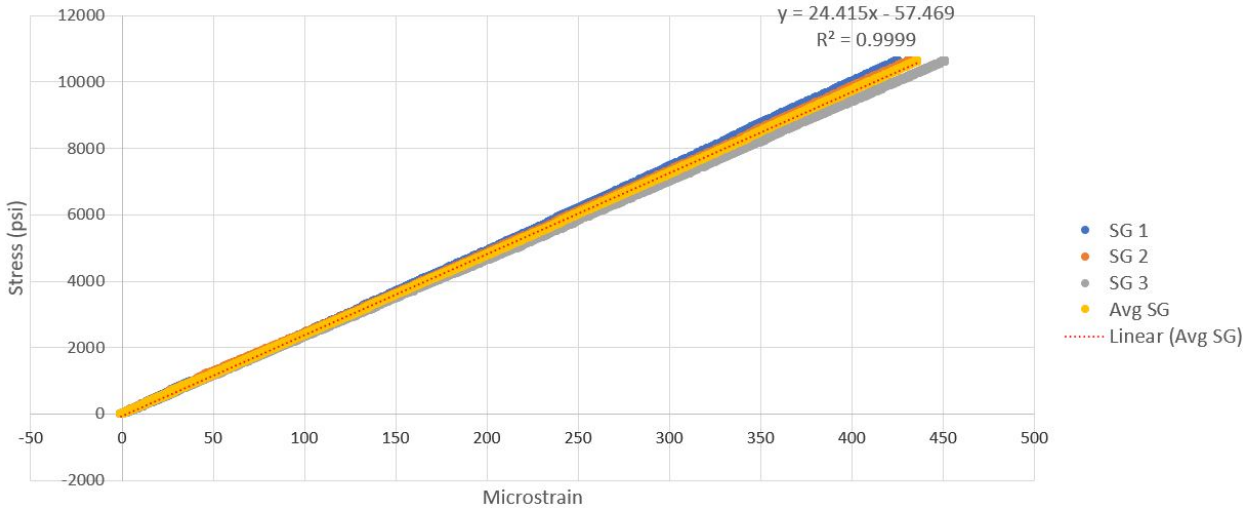

Figure A5: Specimen B, tension trial 2.

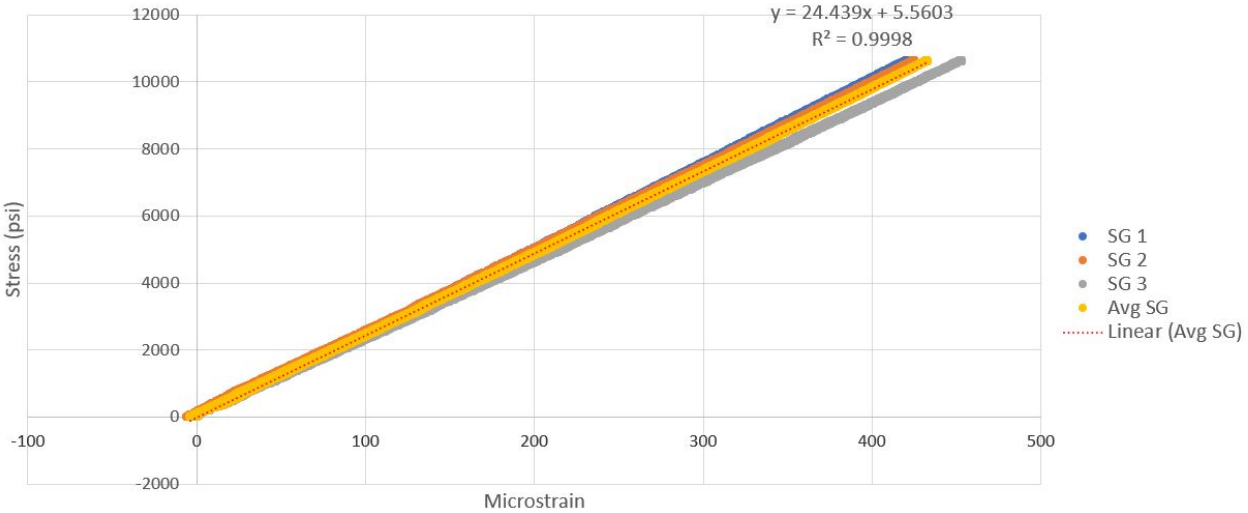

Figure A6: Specimen B, tension trial 3.

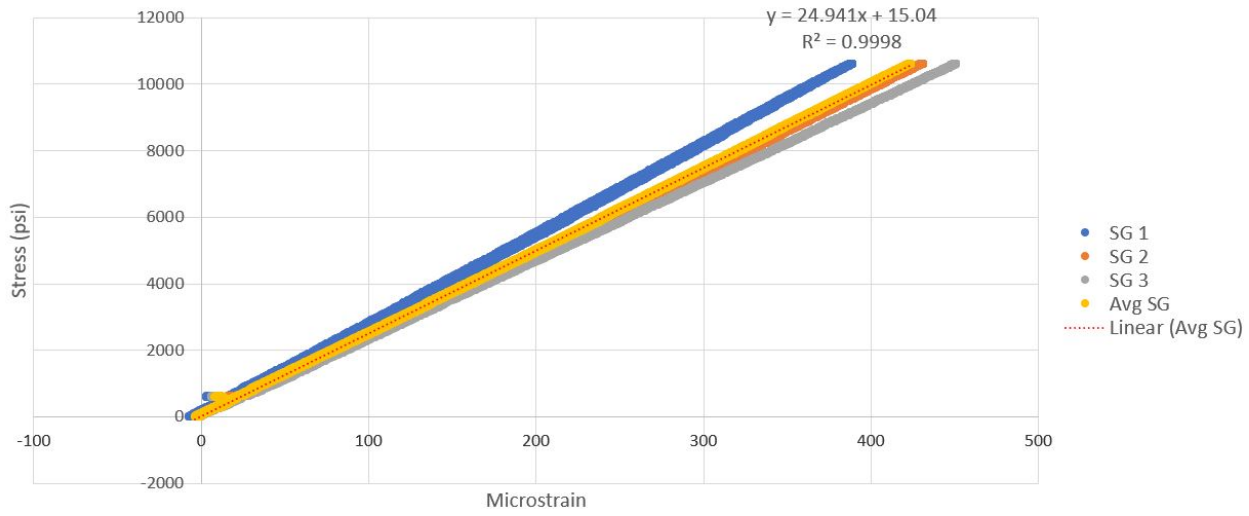

Figure A7: Specimen C, tension trial 1.

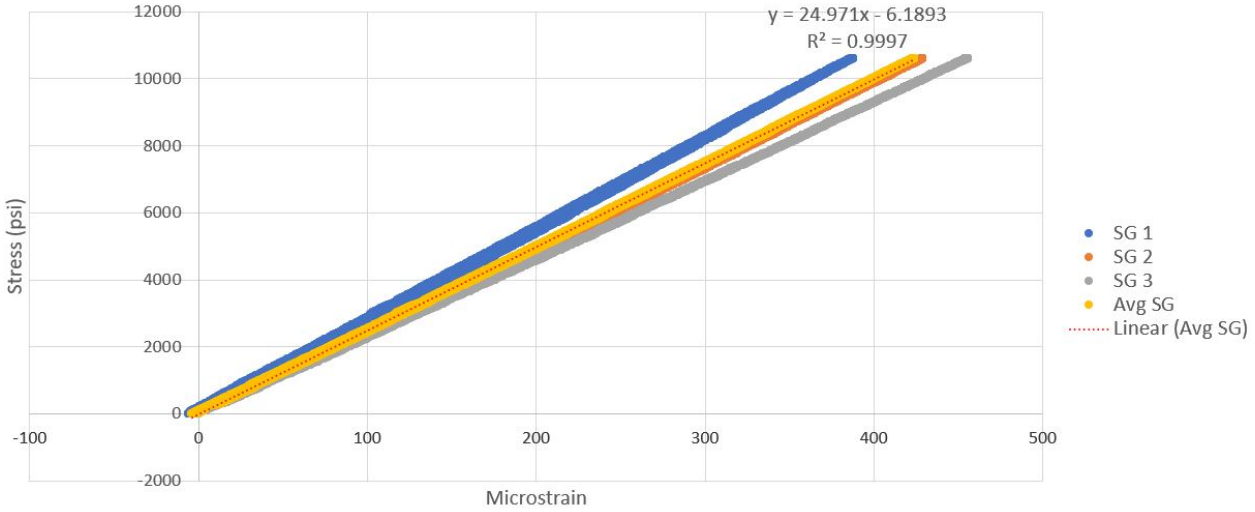

Figure A8: Specimen C, tension trial 2.

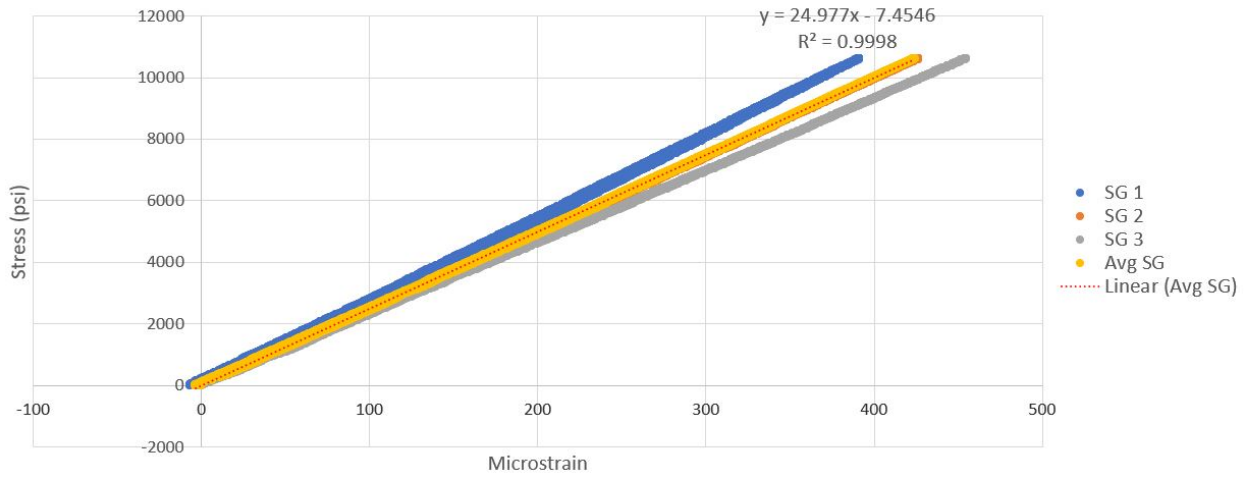

Figure A9: Specimen C, tension trial 3.

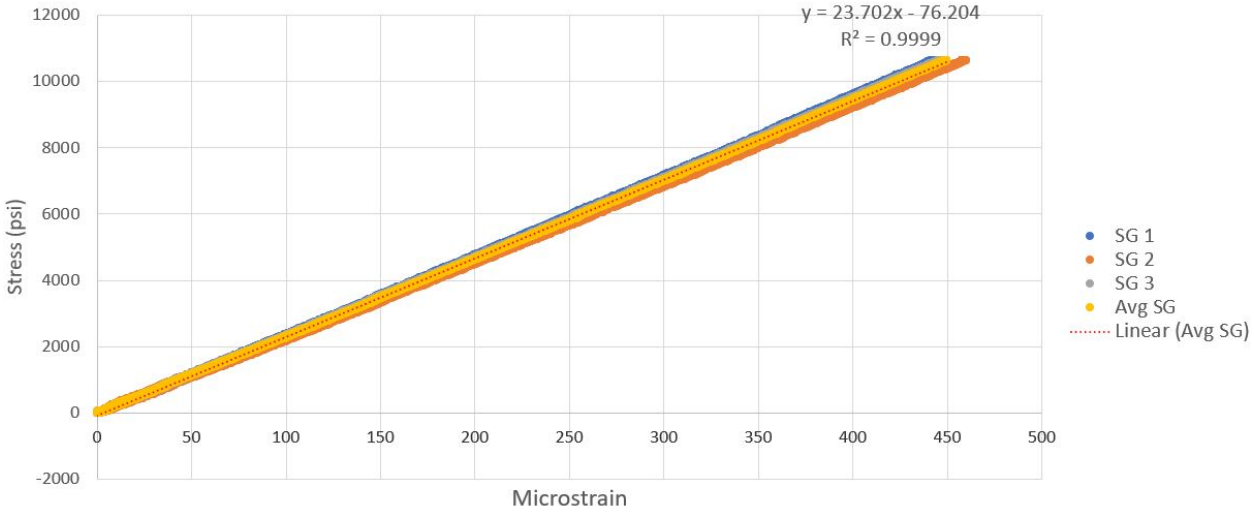

Figure A10: Specimen D, tension trial 1.

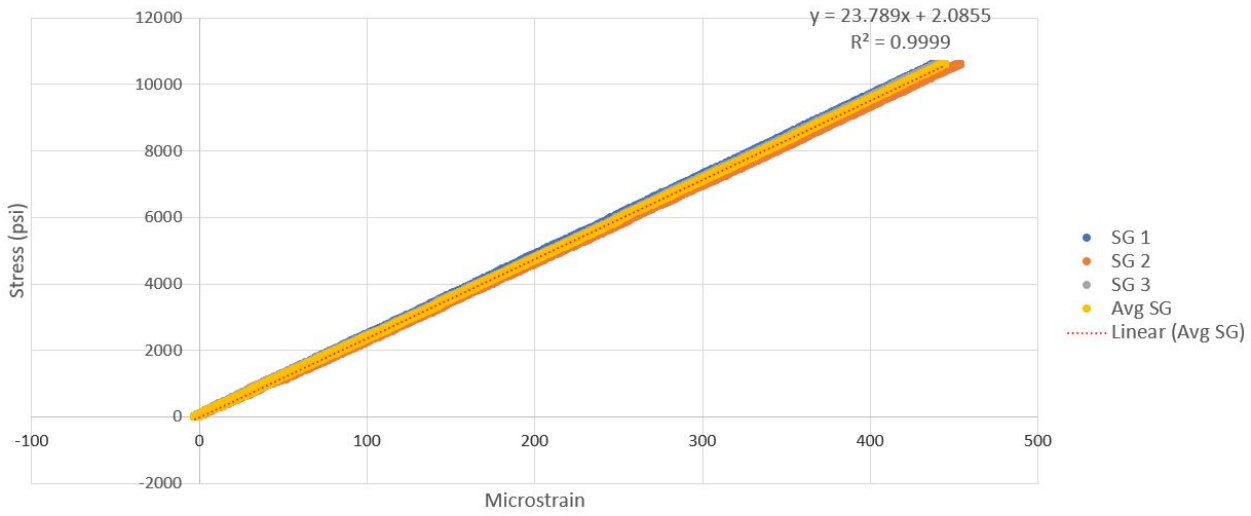

Figure A11: Specimen D, tension trial 2.

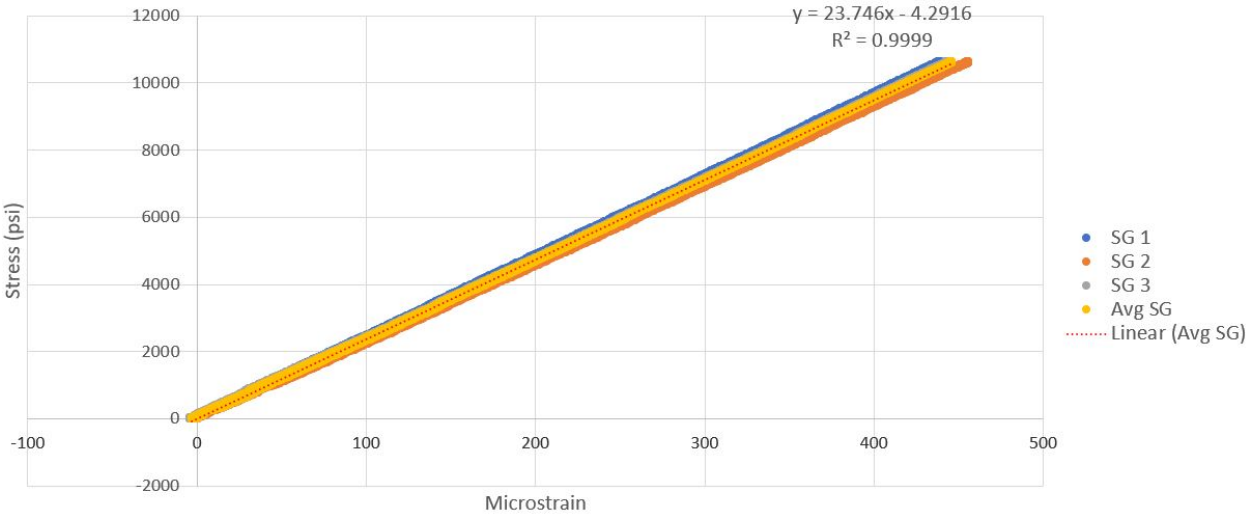

Figure A12: Specimen D, tension trial 3.

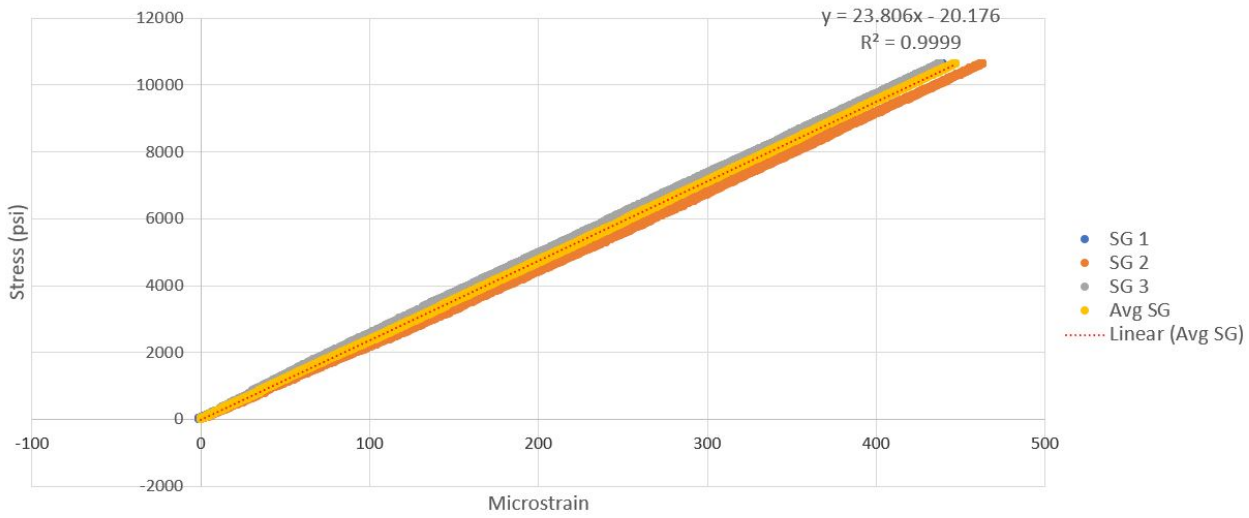

Figure A13: Specimen E, tension trial 1.

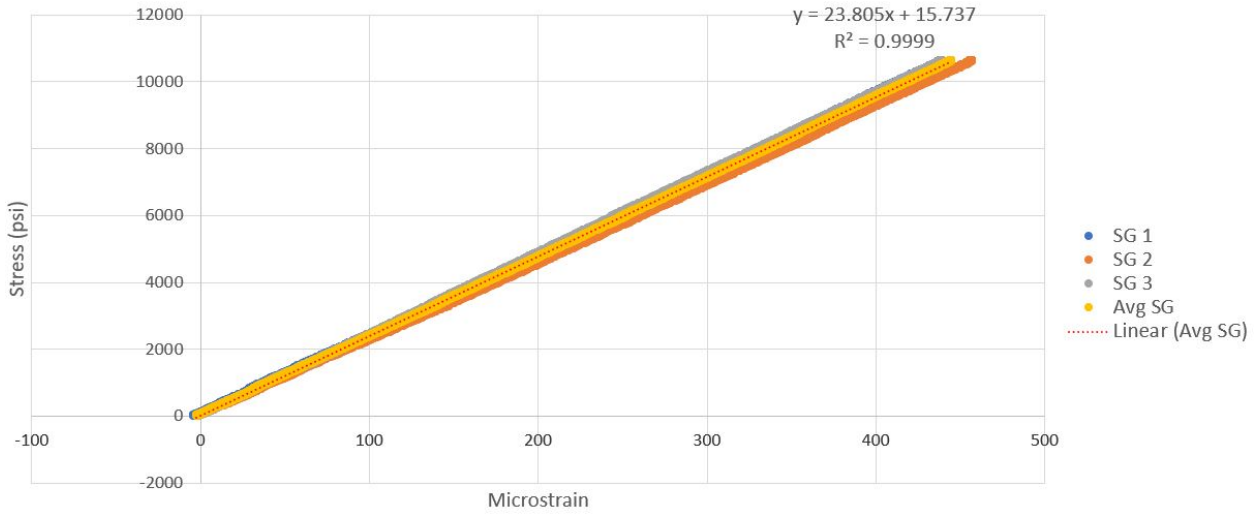

Figure A14: Specimen E, tension trial 2.

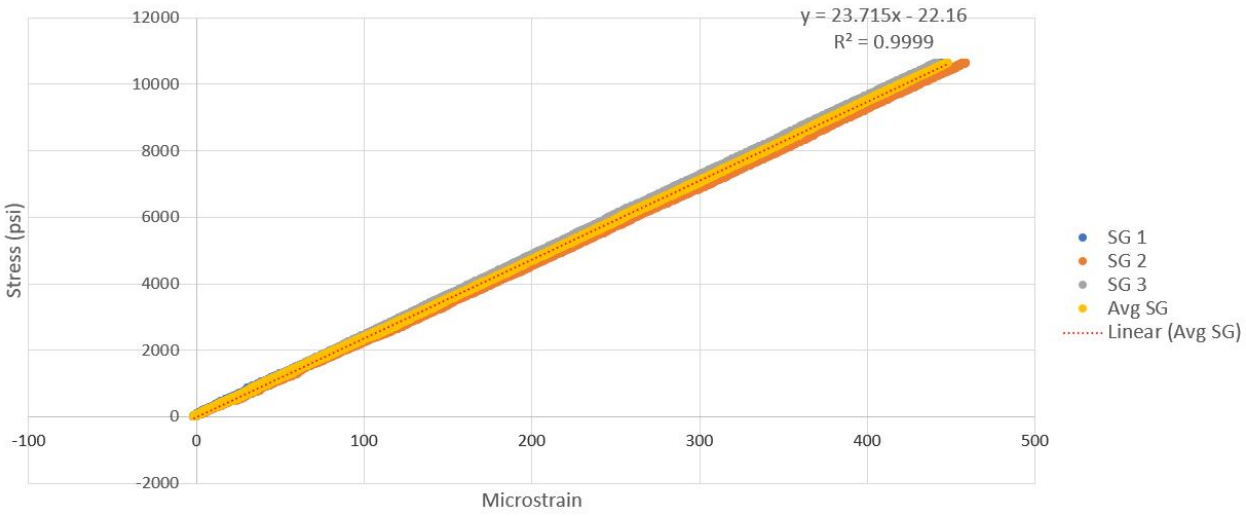

Figure A15: Specimen E, tension trial 3.

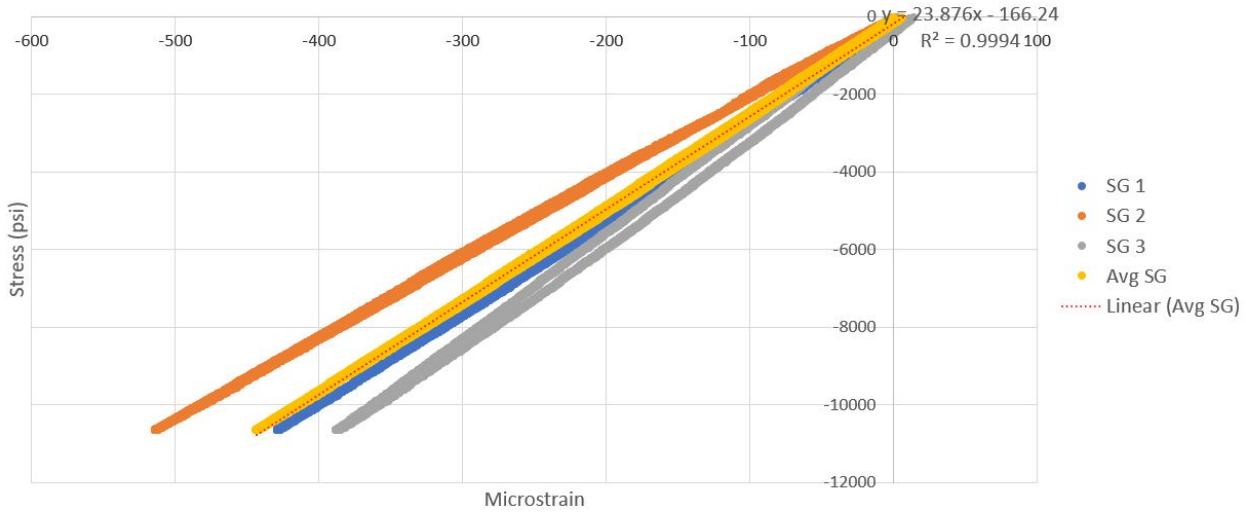

Figure A16: Specimen A, compression trial 1.

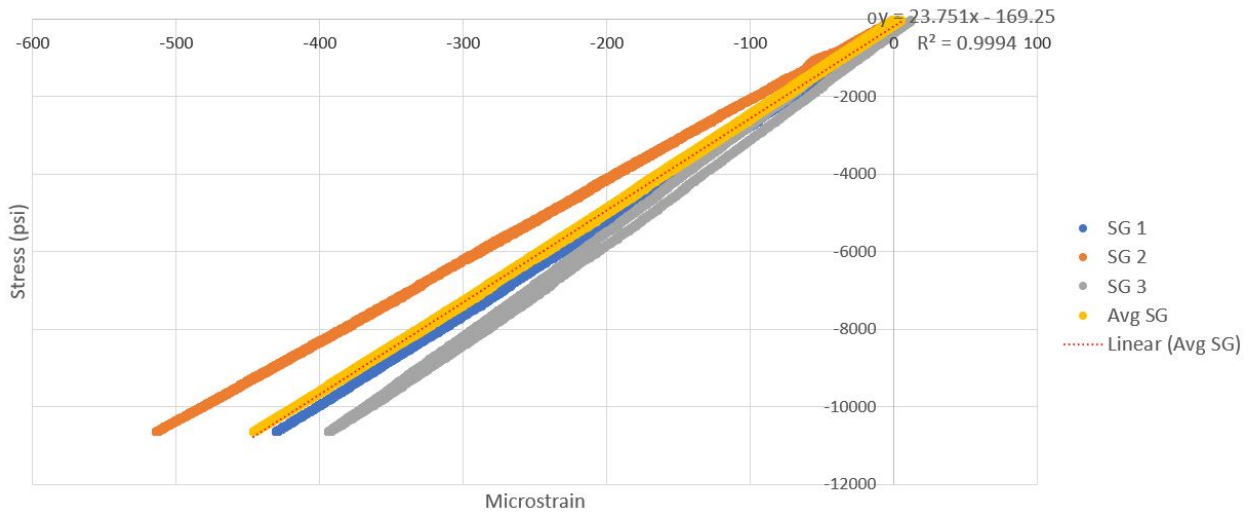

Figure A17: Specimen A, compression trial 2.

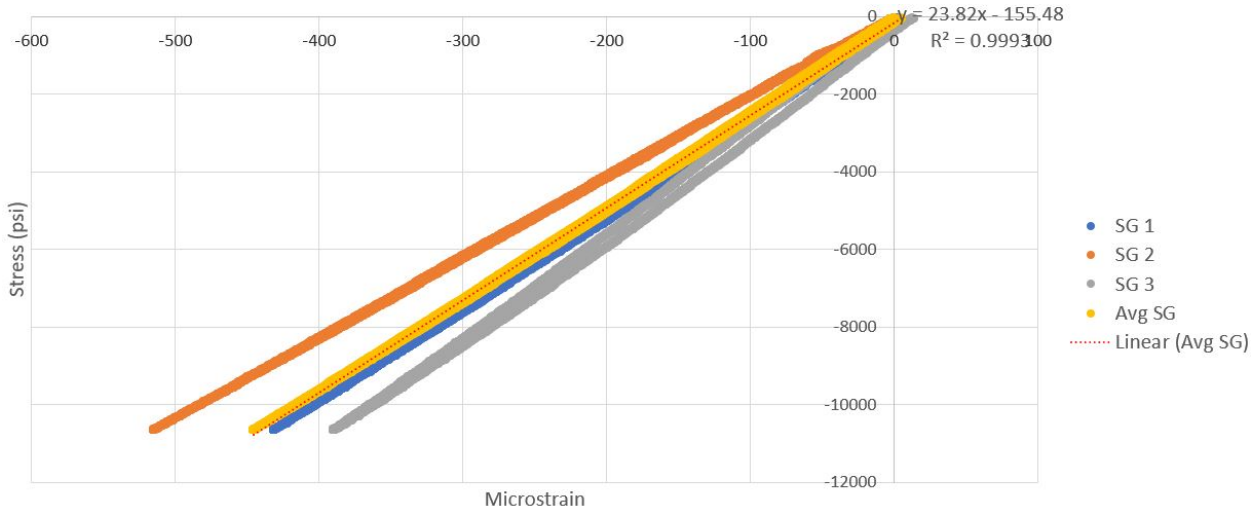

Figure A18: Specimen A, compression trial 3.

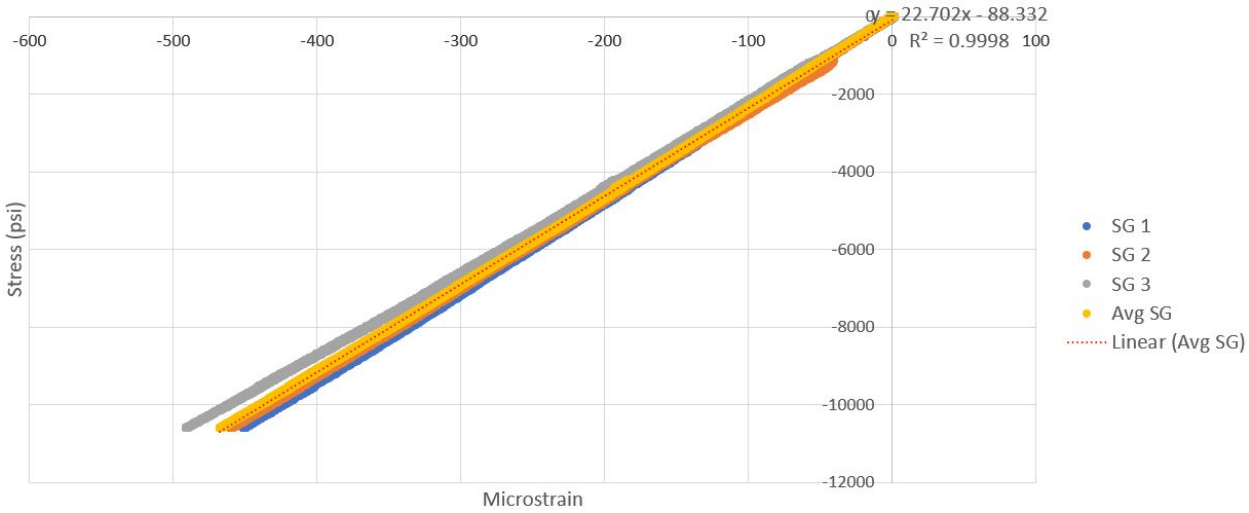

Figure A19: Specimen B, compression trial 1.

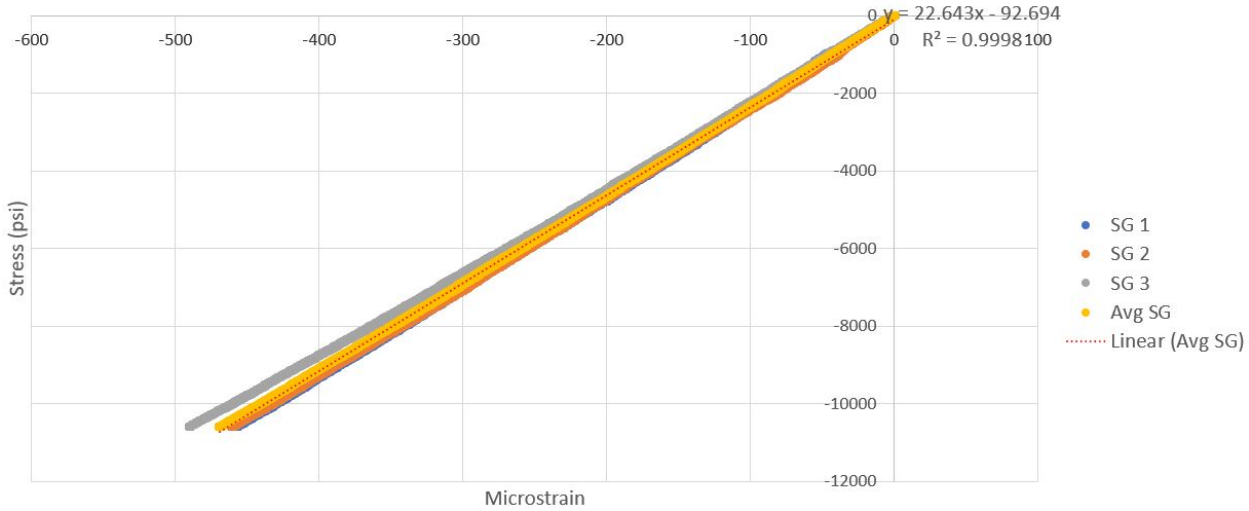

Figure A20: Specimen B, compression trial 2.

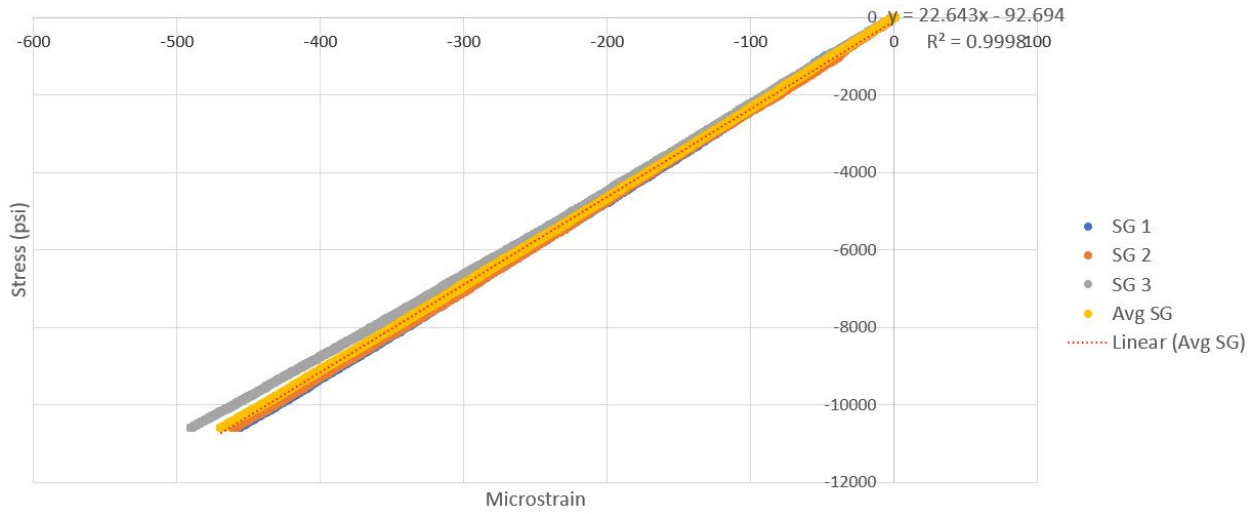

Figure A21: Specimen B, compression trial 3.

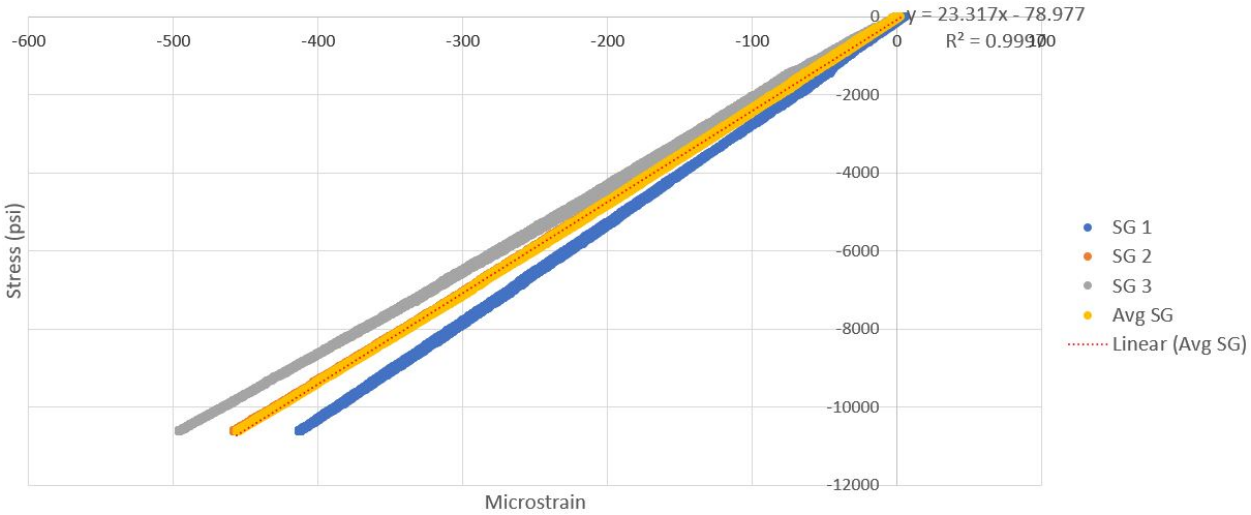

Figure A22: Specimen C, compression trial 1.

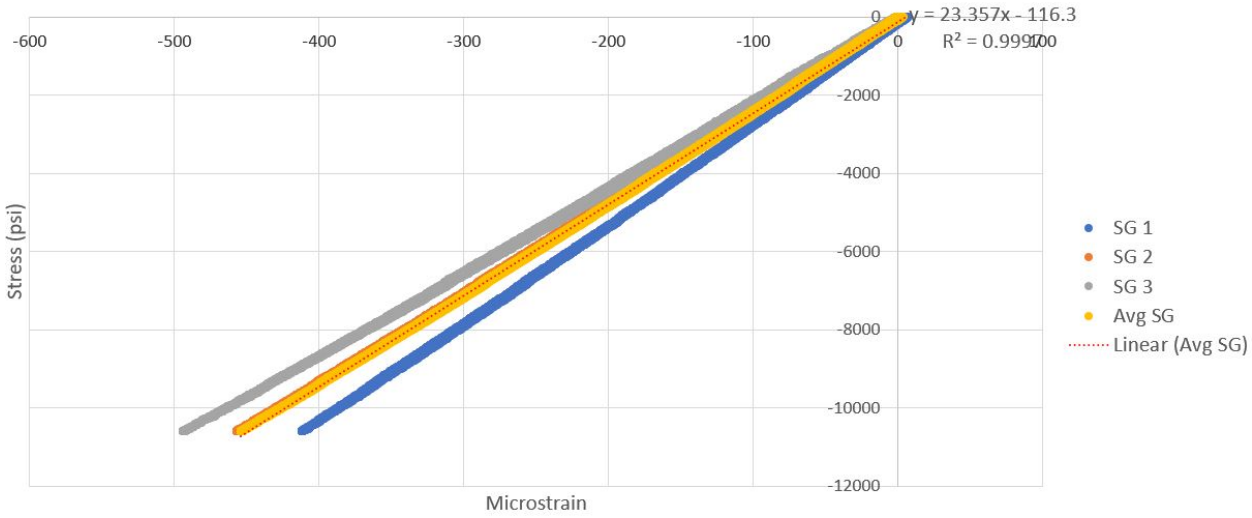

Figure A23: Specimen C, compression trial 2.

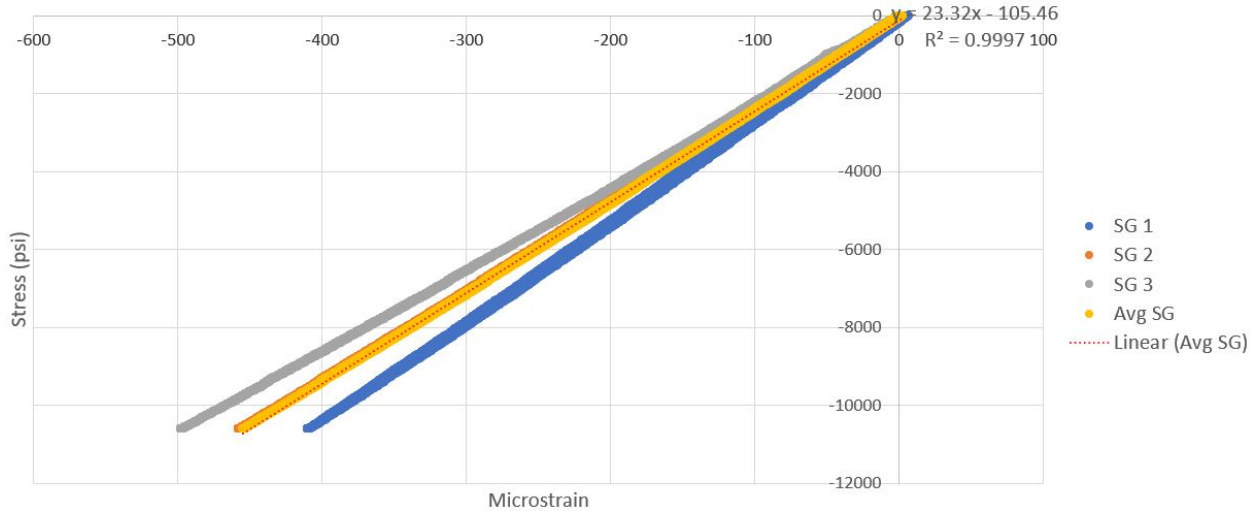

Figure A24: Specimen C, compression trial 3.

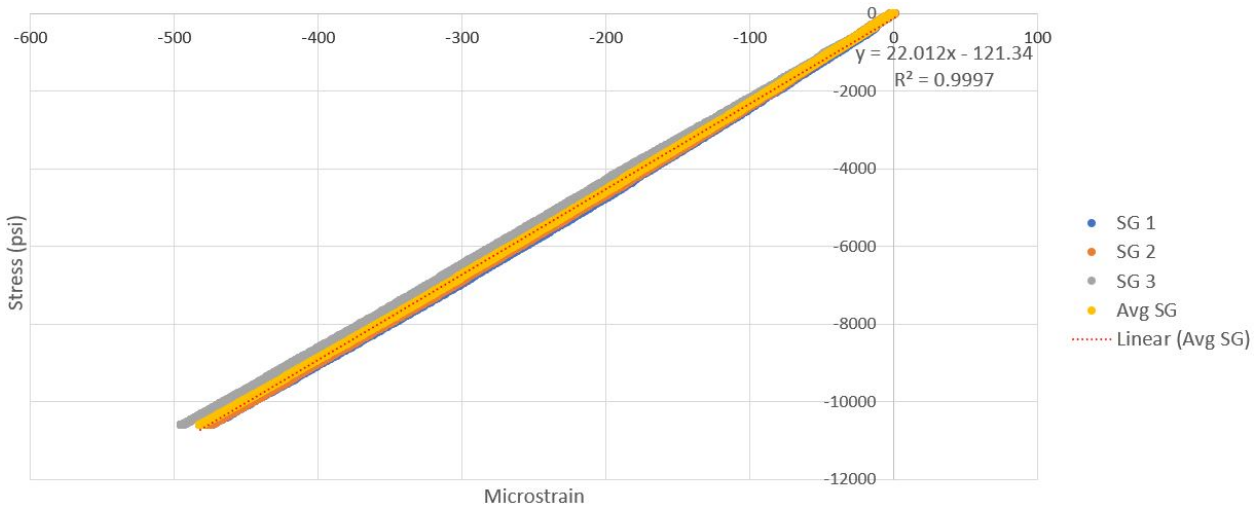

Figure A25: Specimen D, compression trial 1.

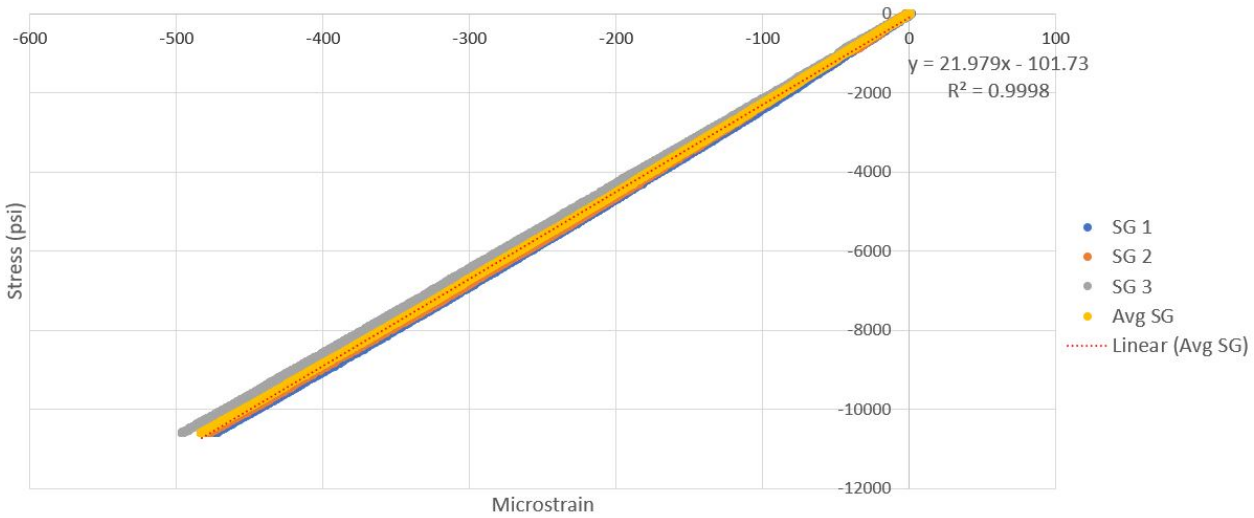

Figure A26: Specimen D, compression trial 2.

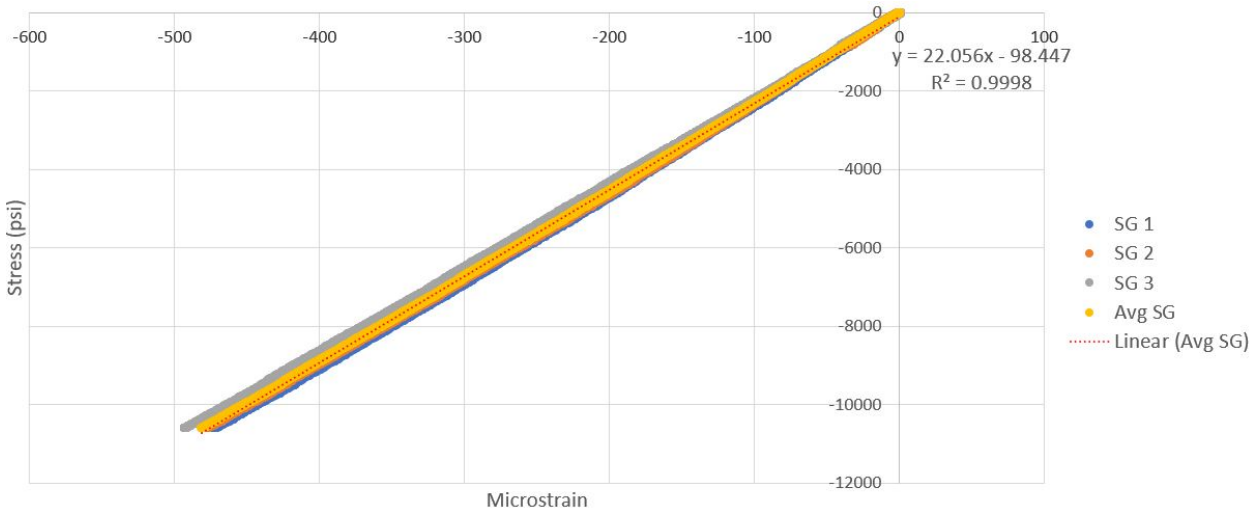

Figure A27: Specimen D, compression trial 3.

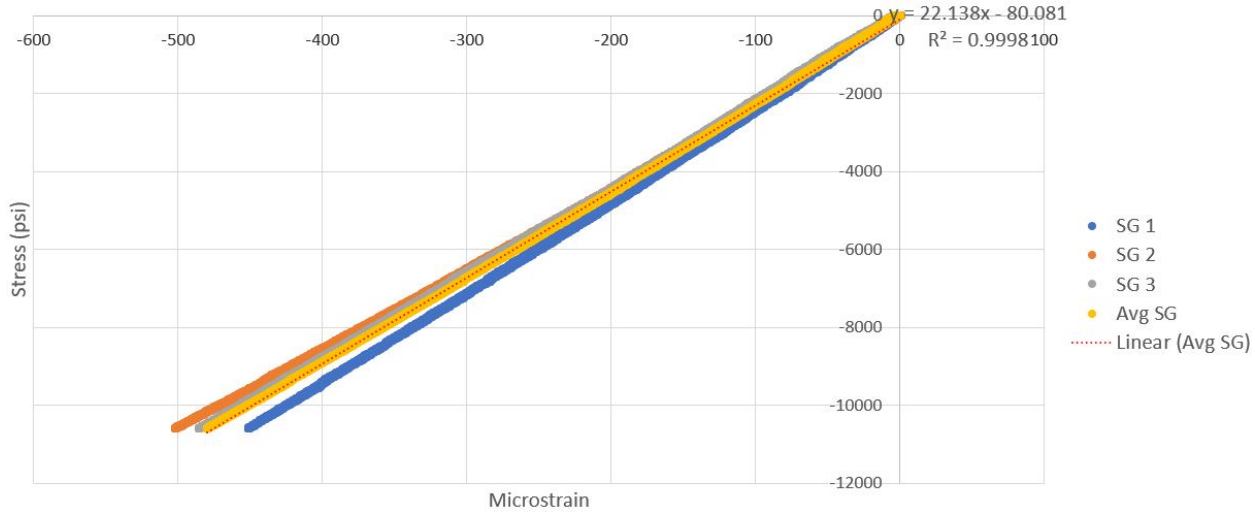

Figure A28: Specimen E, compression trial 1.

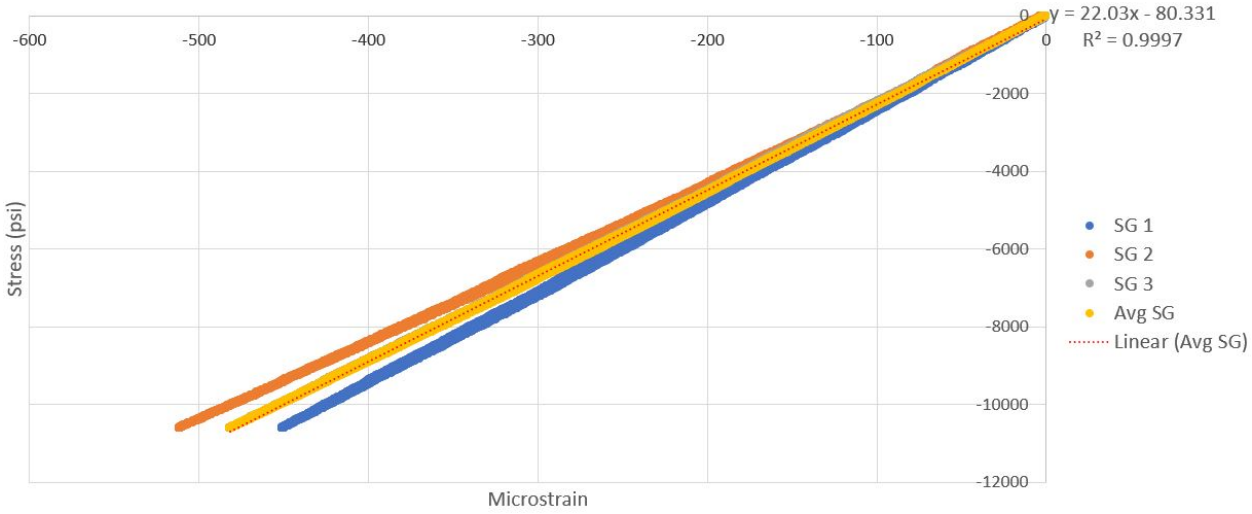

Figure A29: Specimen E, compression trial 2.

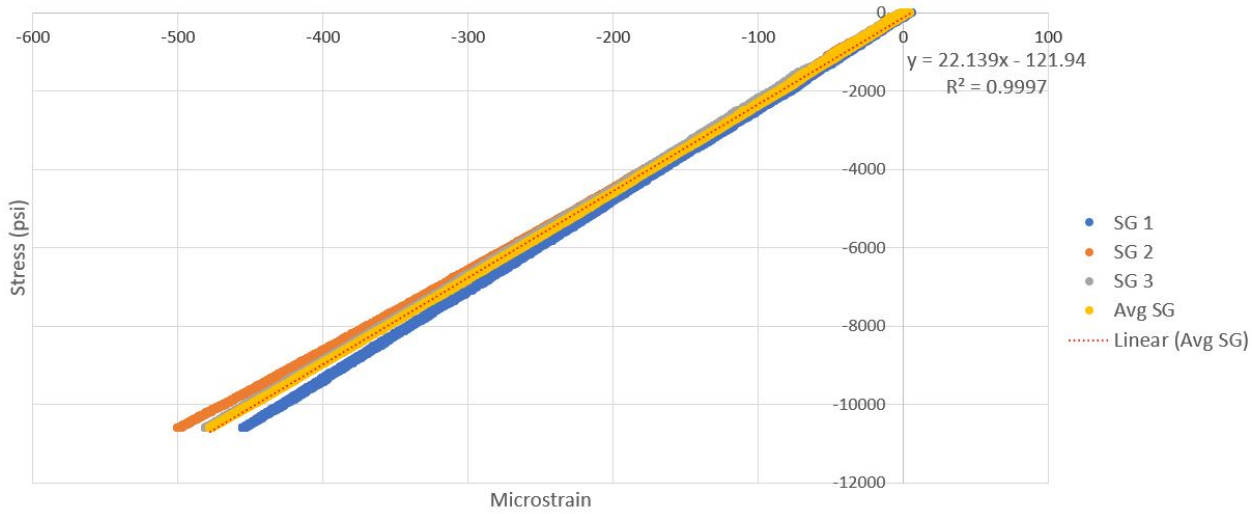

Figure A30: Specimen E, compression trial 3.

Appendix B

Double Wall Thickness Strut Stress vs. Strain Plots

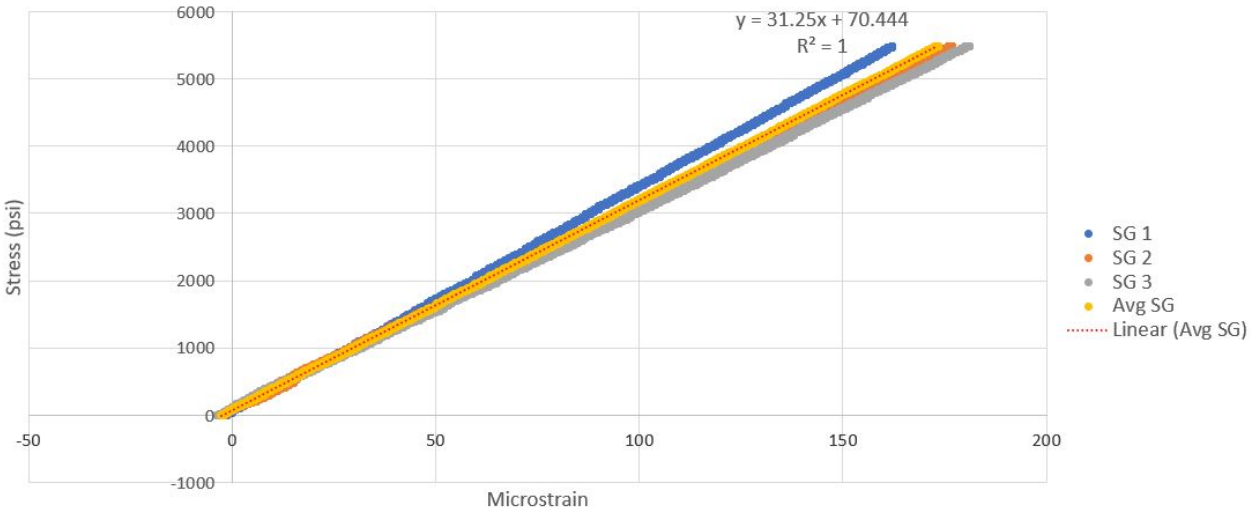

Figure B1: Specimen A, tension trial 1.

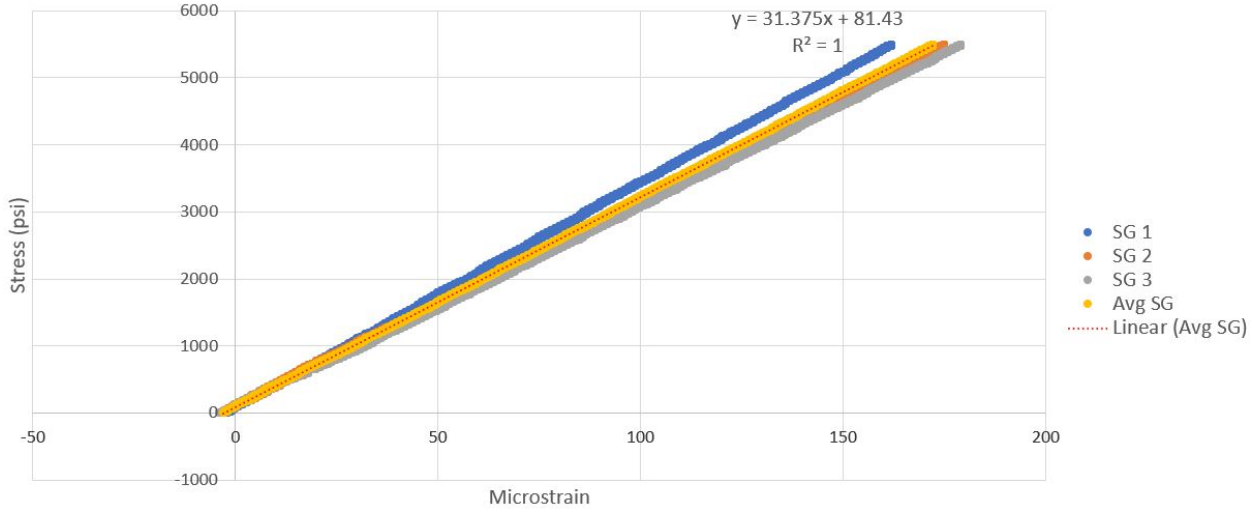

Figure B2: Specimen A, tension trial 2.

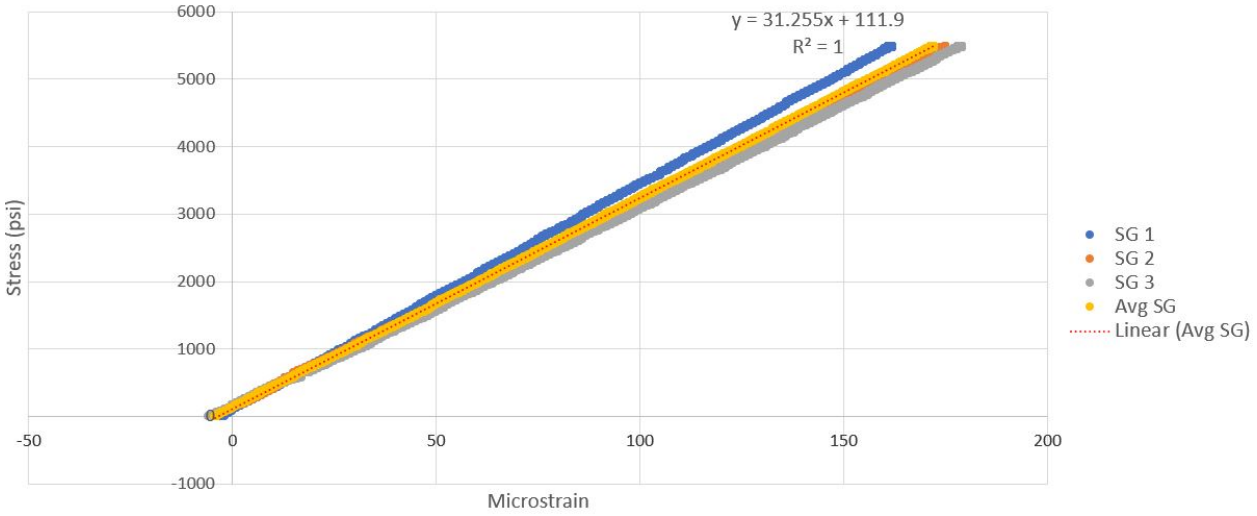

Figure B3: Specimen A, tension trial 3.

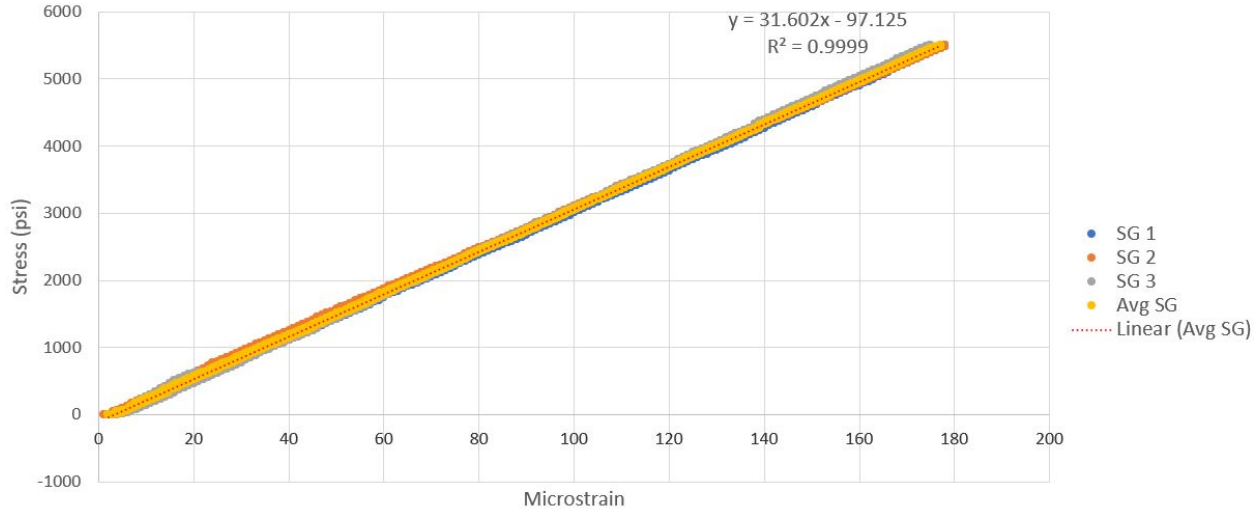

Figure B4: Specimen B, tension trial 1.

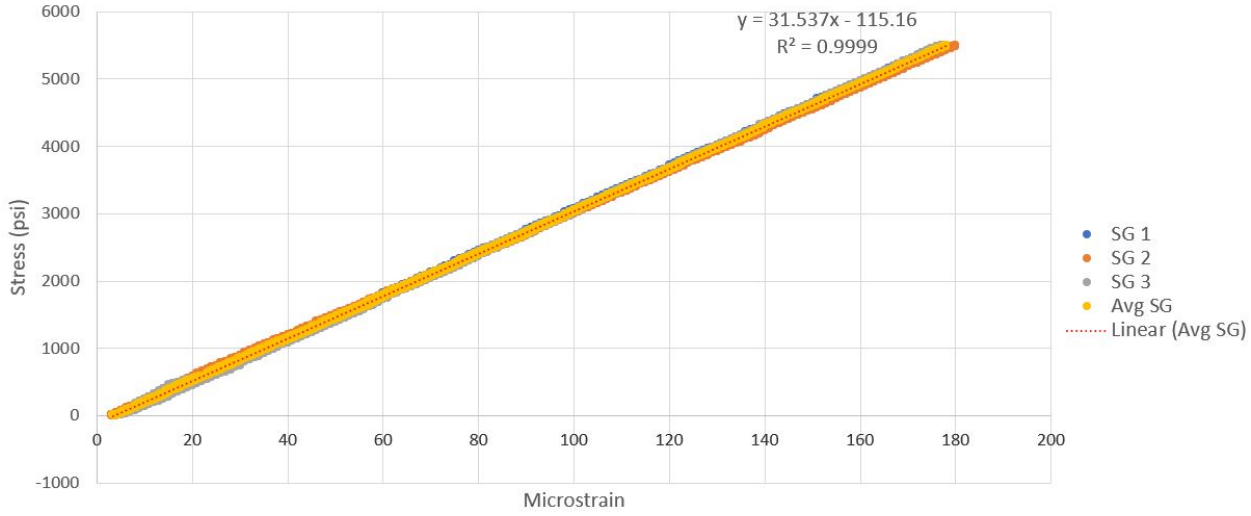

Figure B5: Specimen B, tension trial 2.

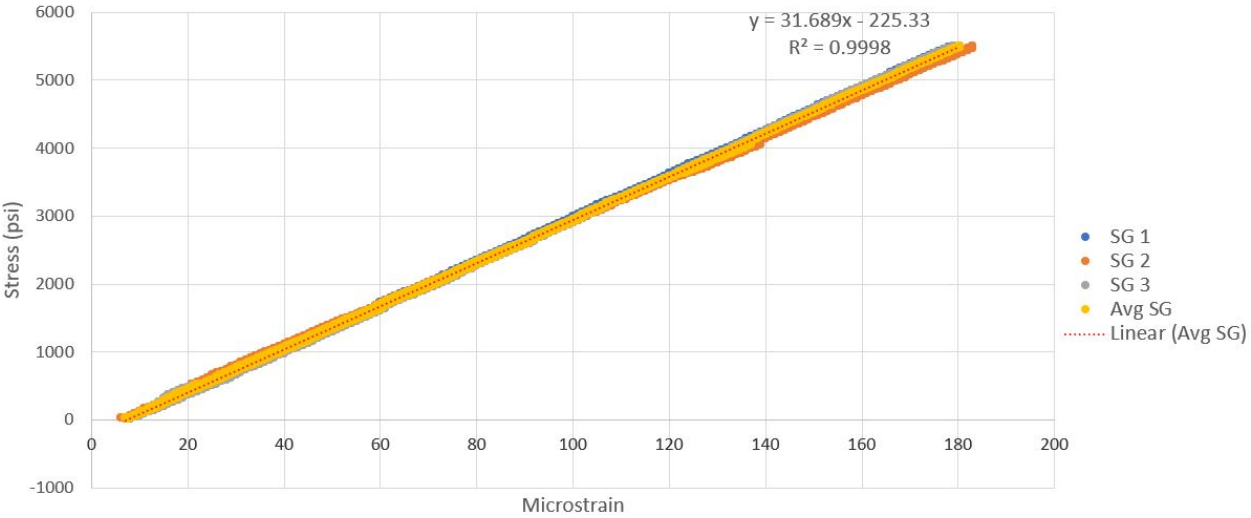

Figure B6: Specimen B, tension trial 3.

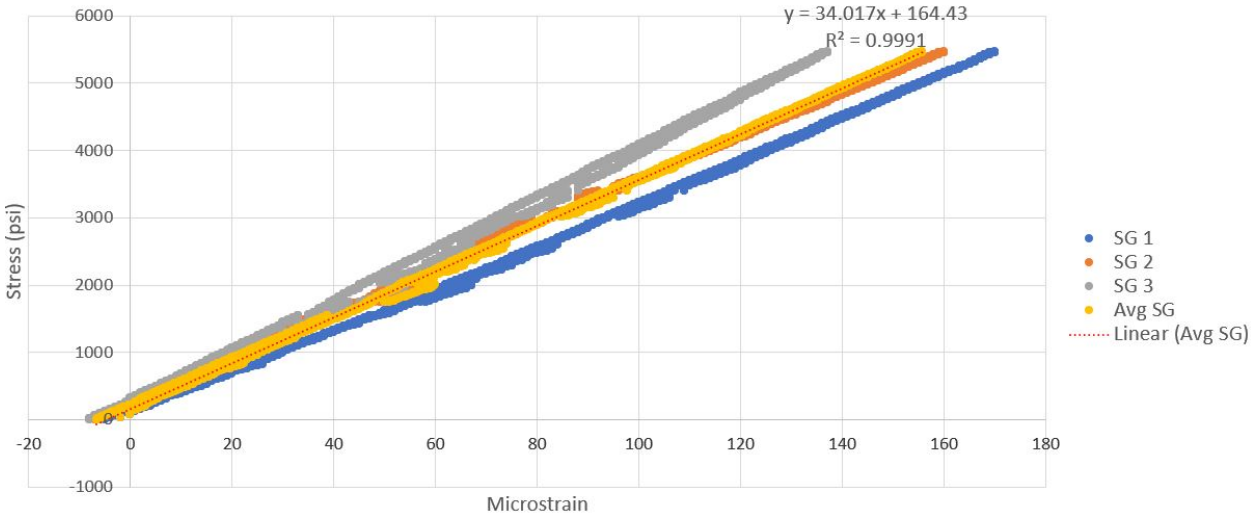

Figure B7: Specimen C, tension trial 1.

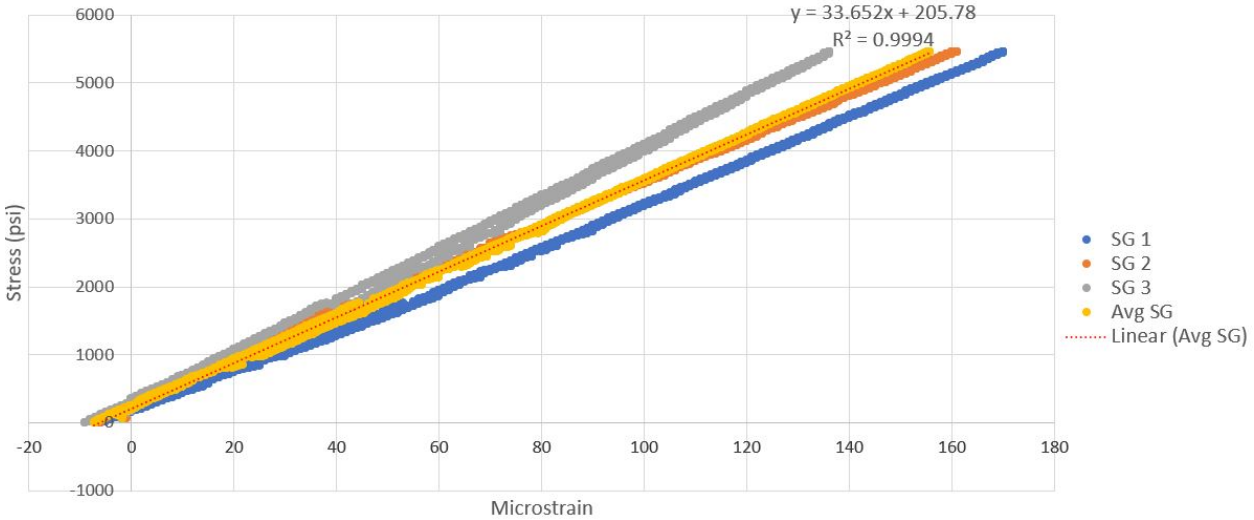

Figure B8: Specimen C, tension trial 2.

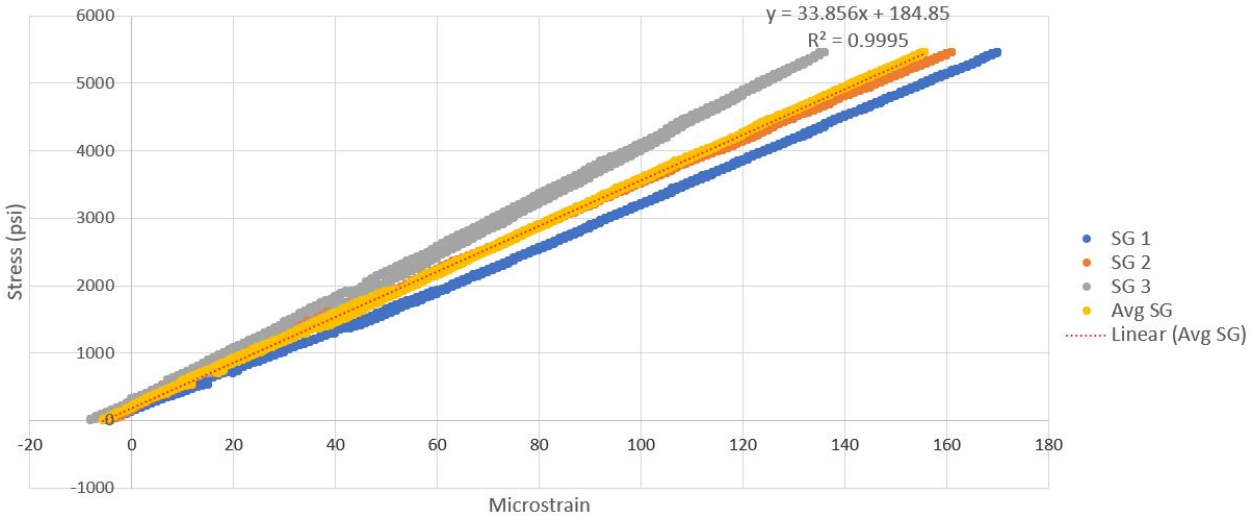

Figure B9: Specimen C, tension trial 3.

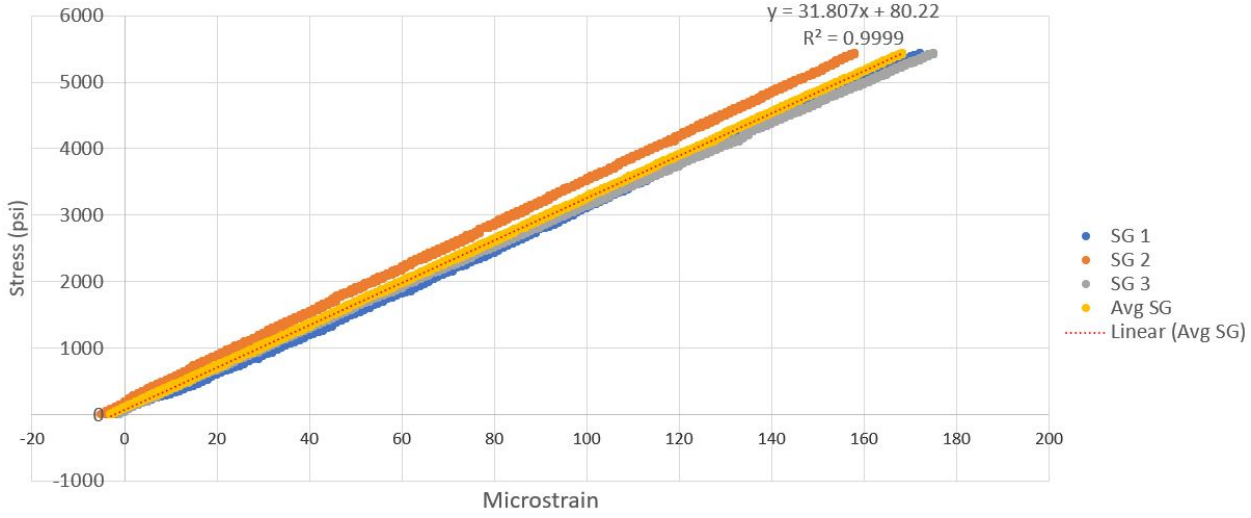

Figure B10: Specimen D, tension trial 1.

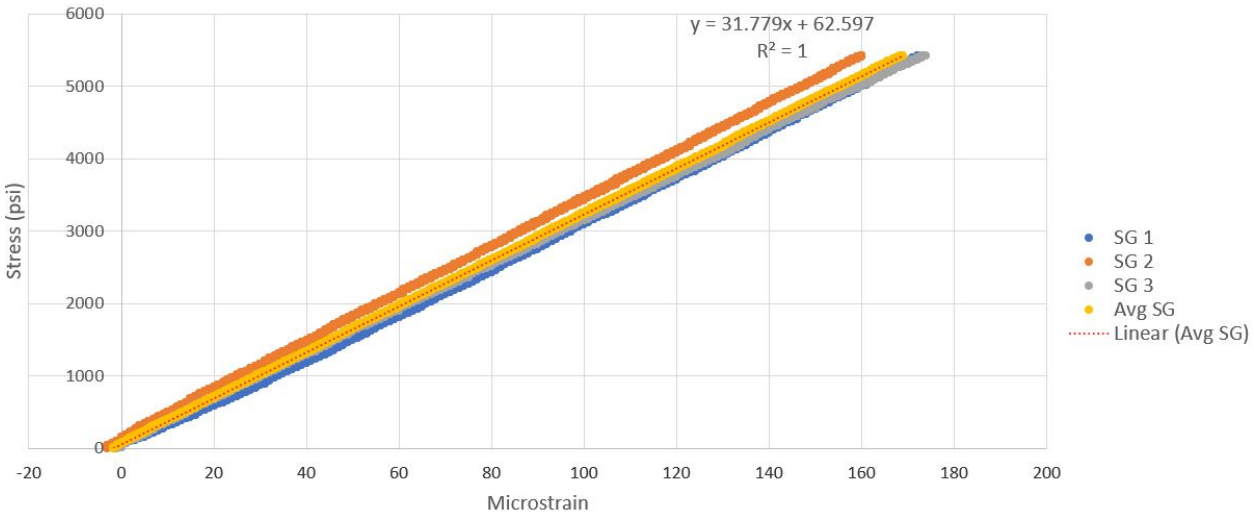

Figure B11: Specimen D, tension trial 2.

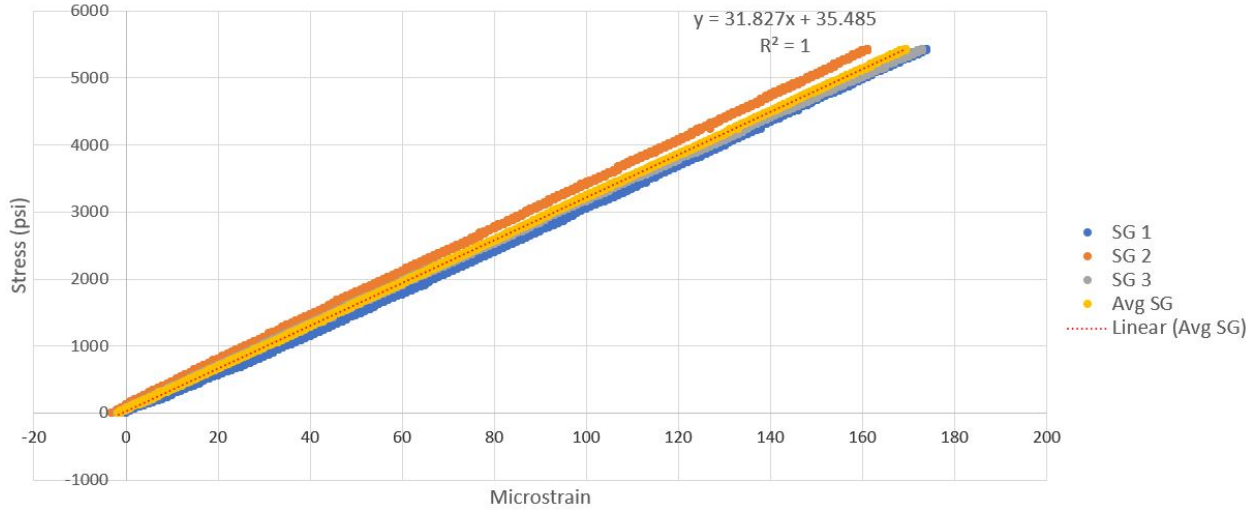

Figure B12: Specimen D, tension trial 3.

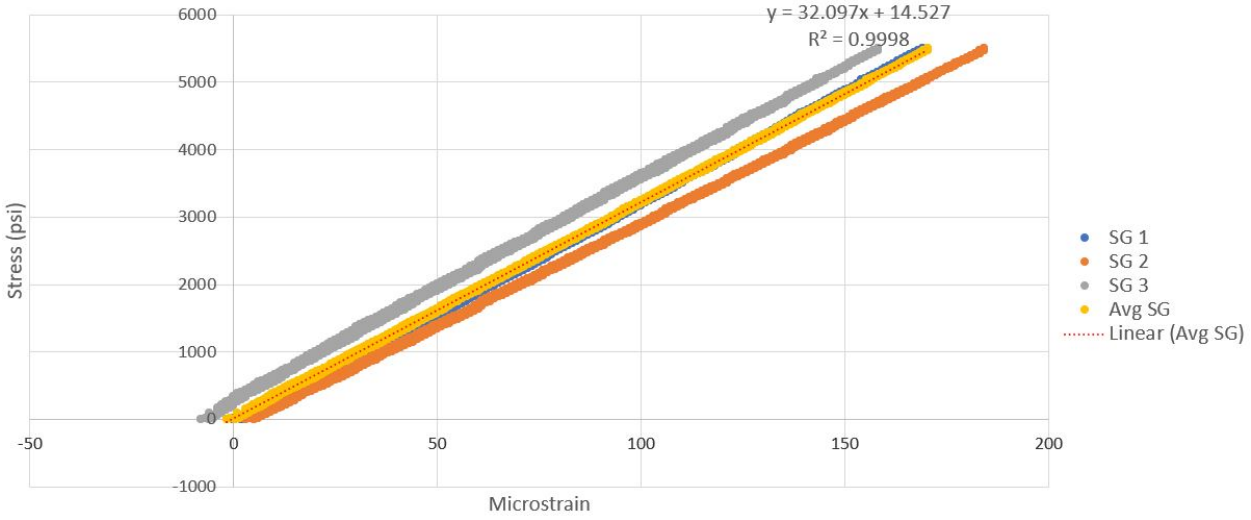

Figure B13: Specimen E, tension trial 1.

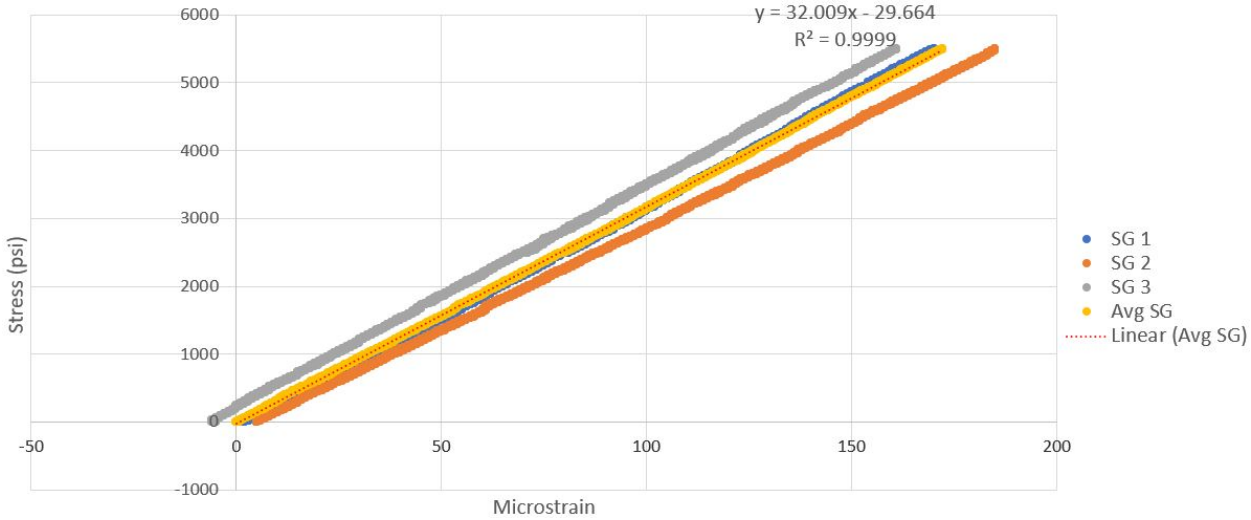

Figure B14: Specimen E, tension trial 2.

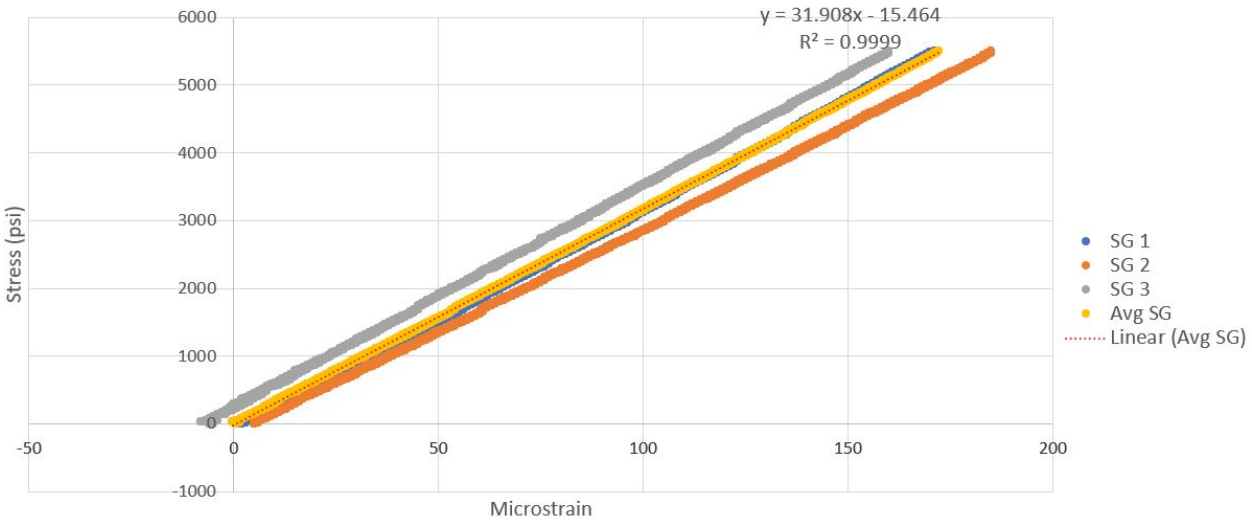

Figure B15: Specimen E, tension trial 3.

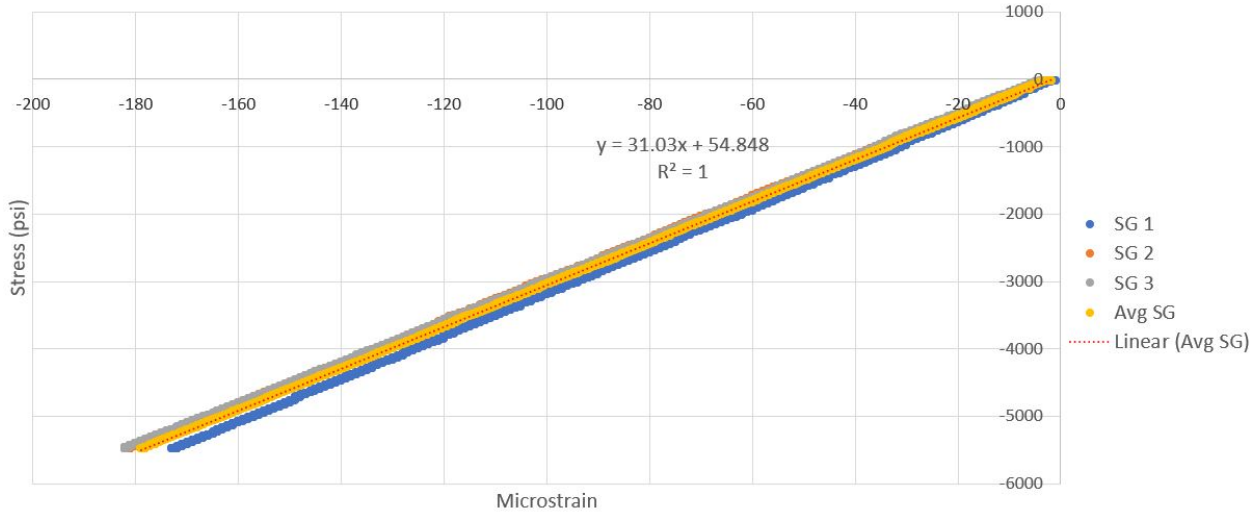

Figure B16: Specimen A, compression trial 1.

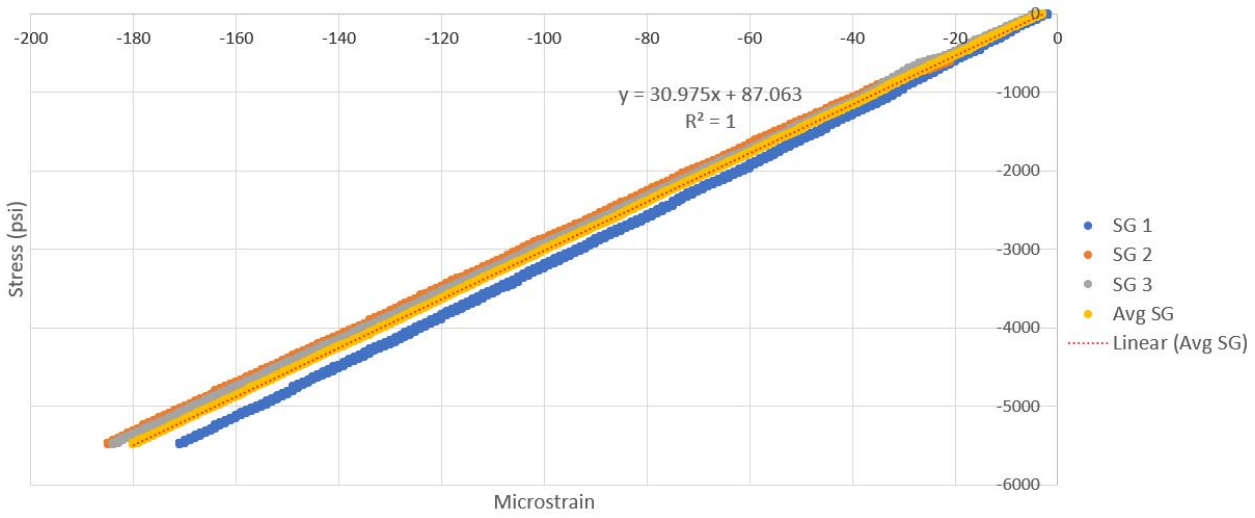

Figure B17: Specimen A, compression trial 2.

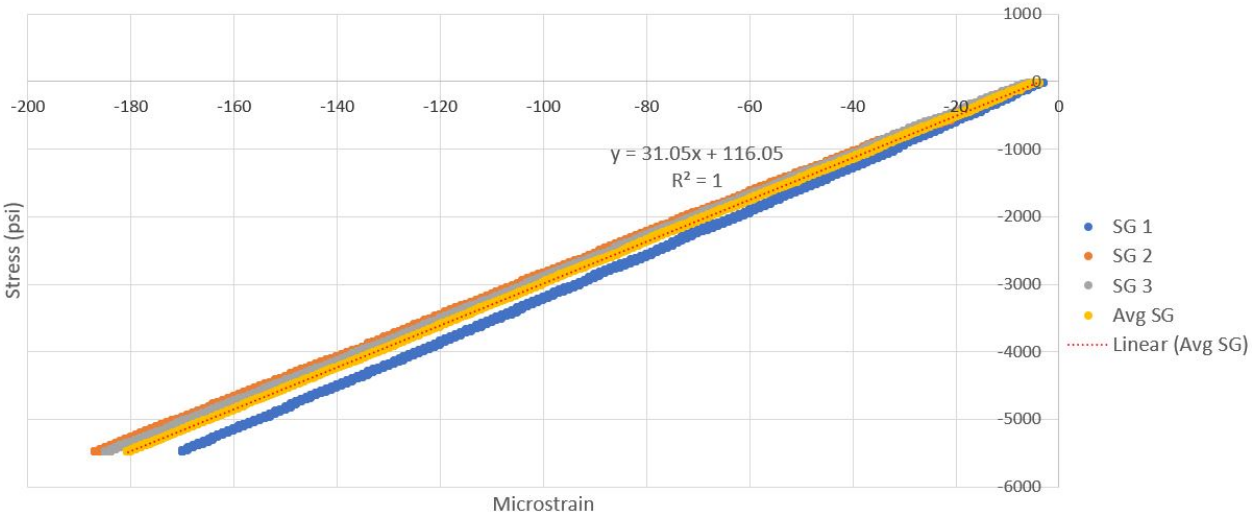

Figure B18: Specimen A, compression trial 3.

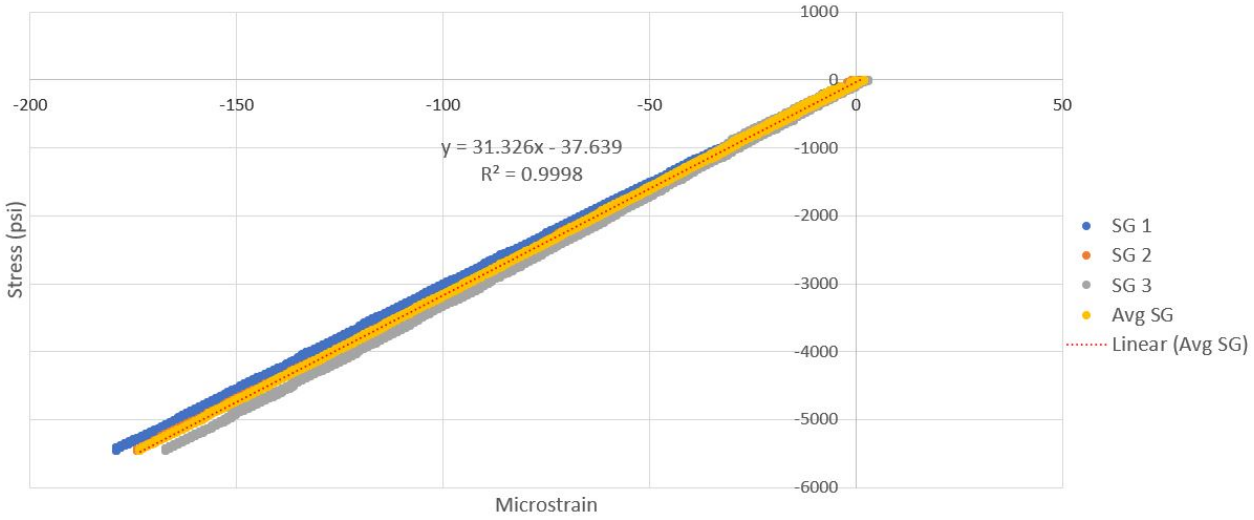

Figure B19: Specimen B, compression trial 1.

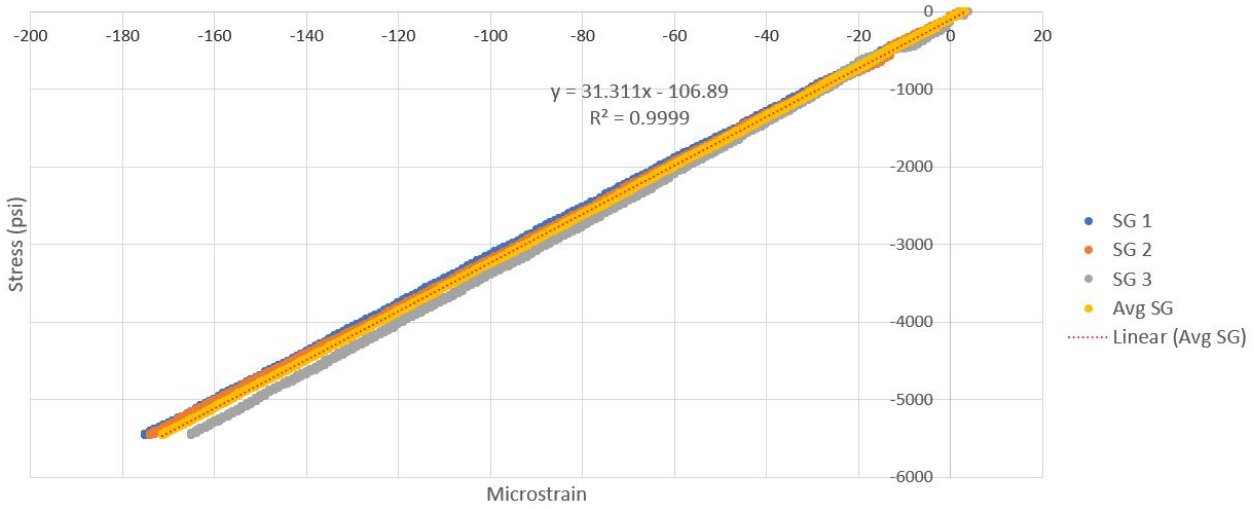

Figure B20: Specimen B, compression trial 2.

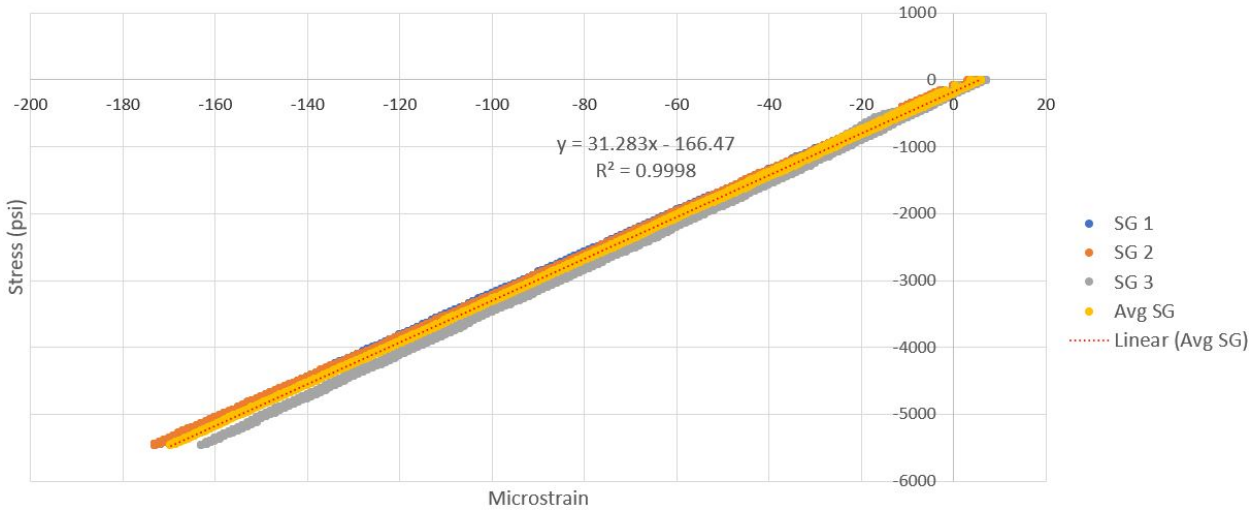

Figure B21: Specimen B, compression trial 3.

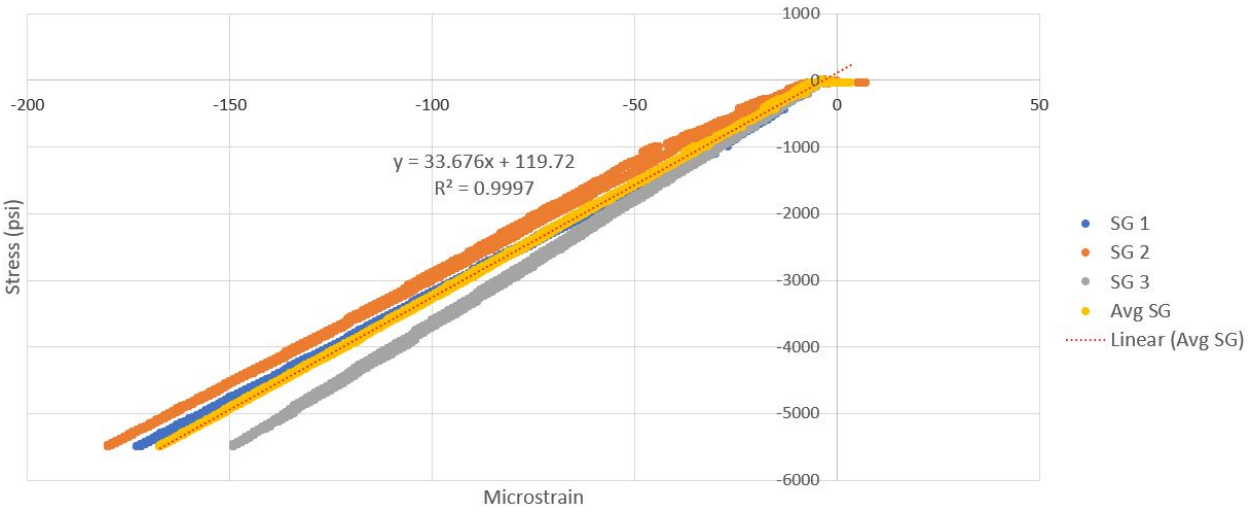

Figure B22: Specimen C, compression trial 1.

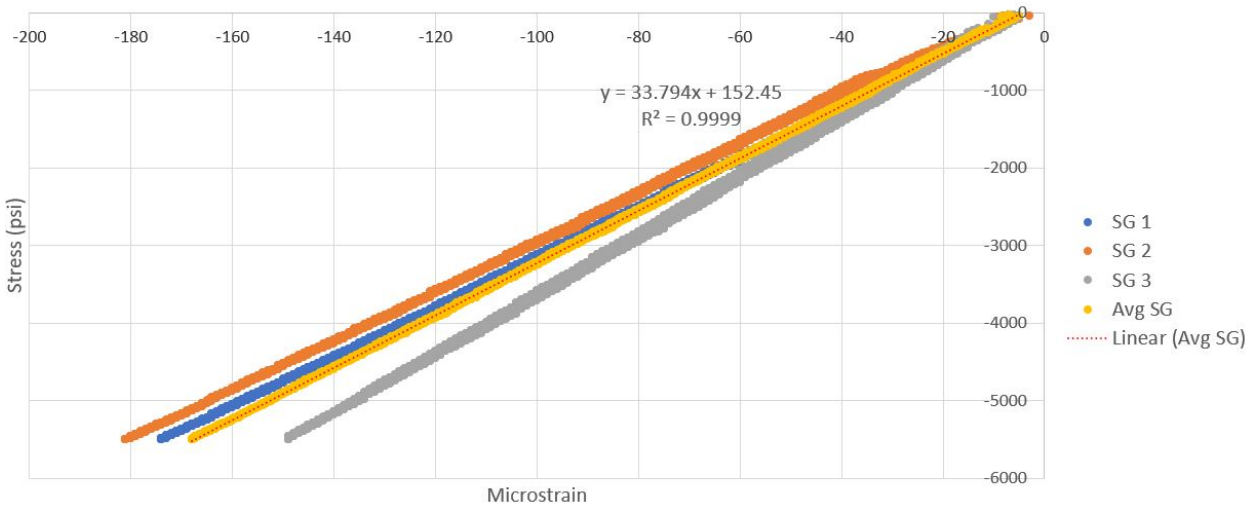

Figure B23: Specimen C, compression trial 2.

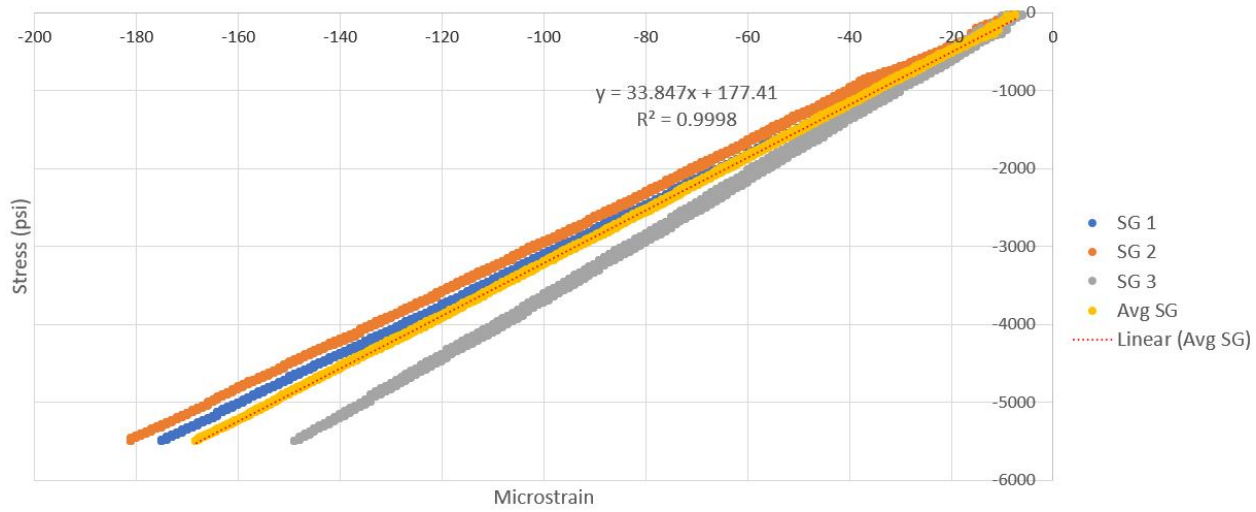

Figure B24: Specimen C, compression trial 3.

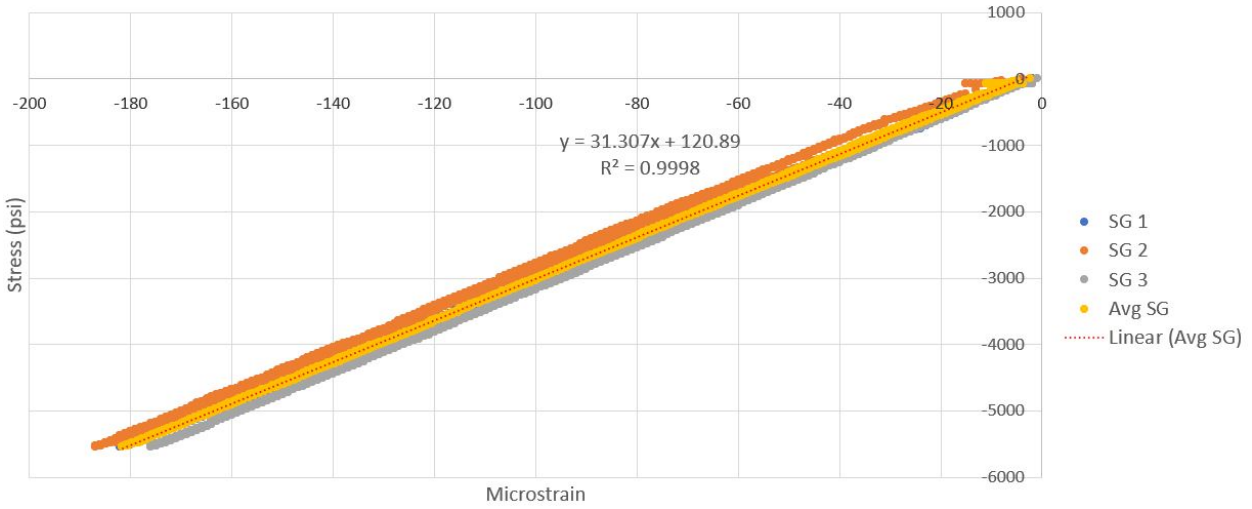

Figure B25: Specimen D, compression trial 1.

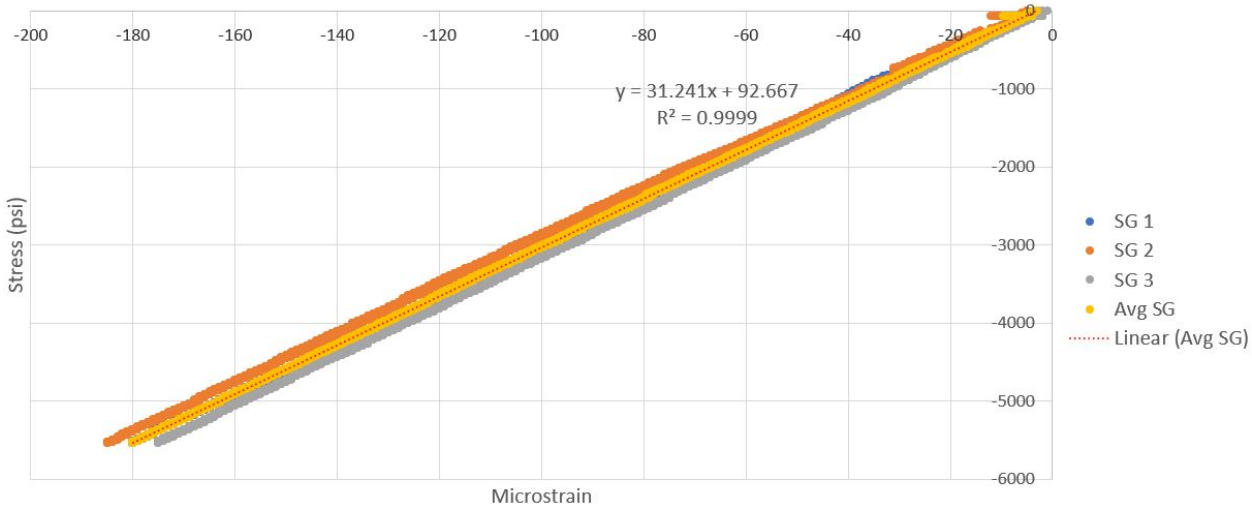

Figure B26: Specimen D, compression trial 2.

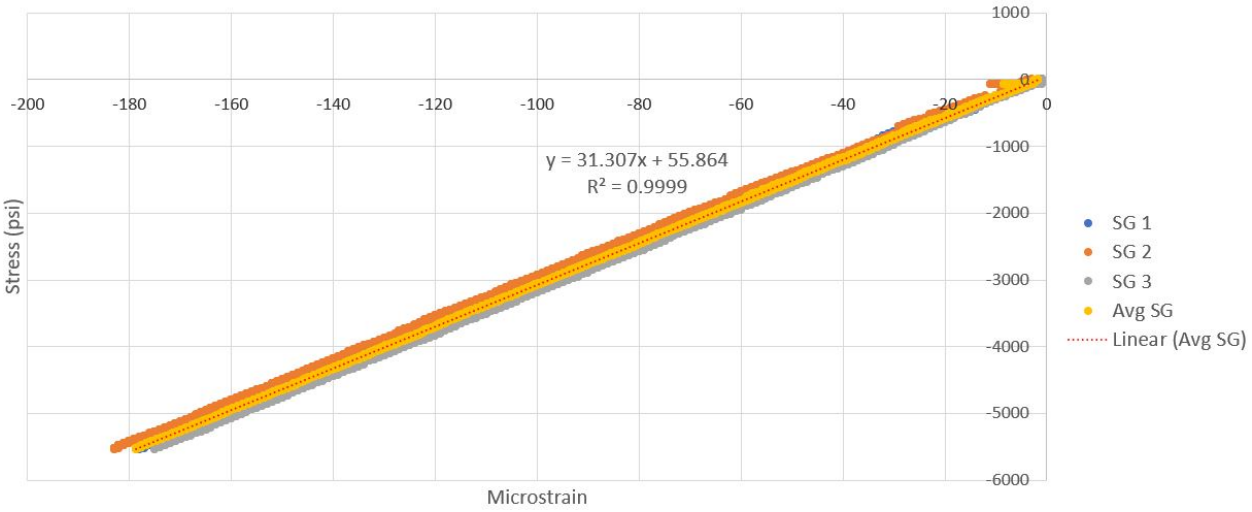

Figure B27: Specimen D, compression trial 3.

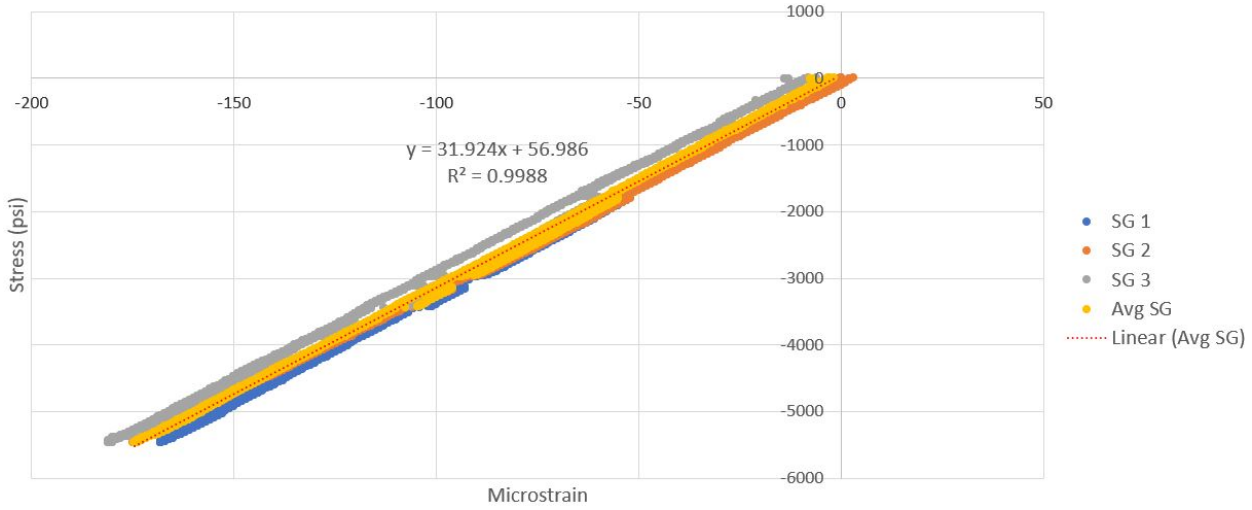

Figure B28: Specimen E, compression trial 1.

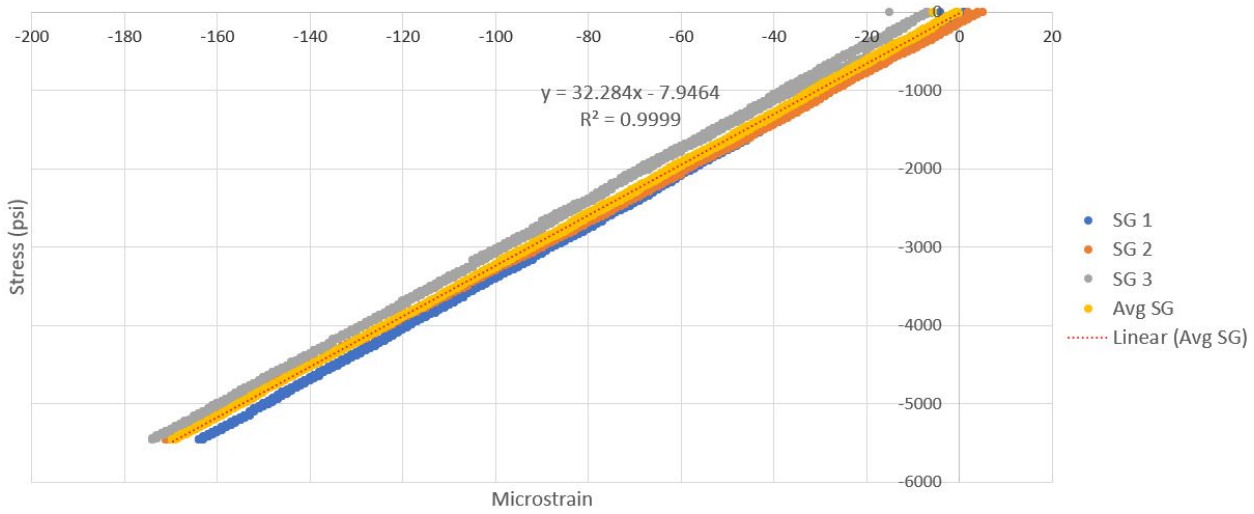

Figure B29: Specimen E, compression trial 2.

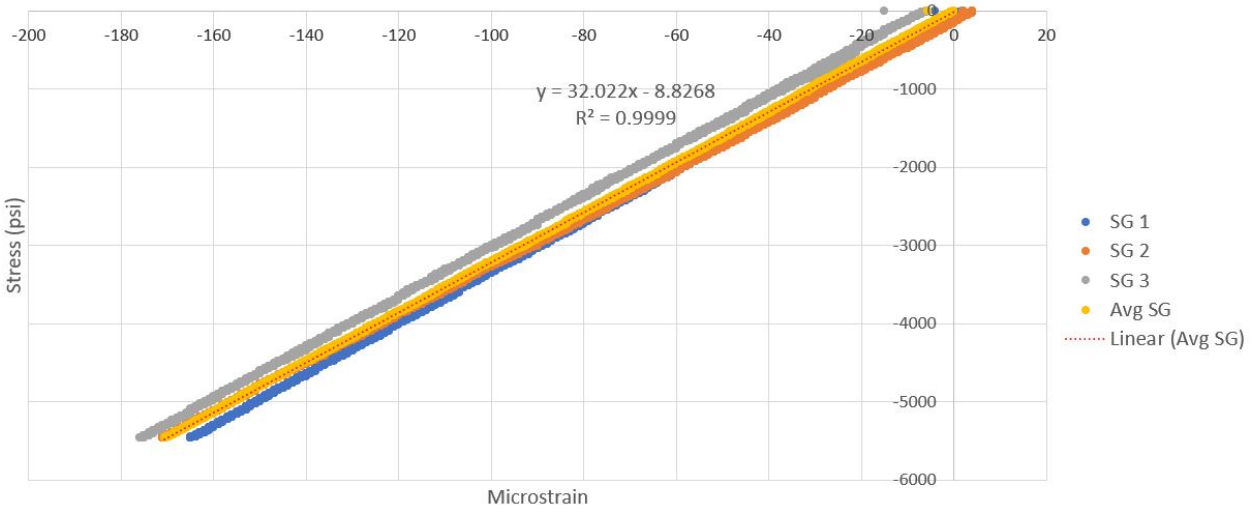

Figure B30: Specimen E, compression trial 3.